

Biostratigraphy and evolution of Miocene *Discoaster* spp. from IODP Site U1338 in the equatorial Pacific Ocean

Marina Ciummelli^{1*}, Isabella Raffi² & Jan Backman³

¹ PetroStrat Ltd, Tan-y-Graig, Parc Caer Seion, Conwy LL32 8FA, UK

² Dipartimento di Ingegneria e Geologia, Università 'G. d'Annunzio' di Chieti-Pescara, I-66013 Chieti Scalo, Italy

³ Department of Geological Sciences, Stockholm University, SE-106 91 Stockholm, Sweden

* Correspondence: marina.ciummelli@petrostrat.com

Abstract: Assemblages of upper lower through upper Miocene *Discoaster* spp. have been quantified from Integrated Ocean Drilling Program (IODP) Site U1338 in the eastern equatorial Pacific Ocean. These assemblages can be grouped into five broad morphological categories: six-rayed with bifurcated ray tips, six-rayed with large central areas, six-rayed with pointed ray tips, five-rayed with bifurcated ray tips and five-rayed with pointed ray tips. *Discoaster deflandrei* dominates the assemblages prior to 15.8 Ma. The decline in abundance of *D. deflandrei* close to the early–middle Miocene boundary occurs together with the evolution of the *D. variabilis* group, including *D. signus* and *D. exilis*. Six-rayed discoasters having large central areas become a prominent member of the assemblages for a 400 ka interval in the late middle Miocene. Five- and six-rayed forms having pointed tips become prominent in the early late Miocene and show a strong antiphasing relationship with the *D. variabilis* group. *Discoaster bellus* completely dominates the *Discoaster* assemblages for a 400 ka interval in the middle late Miocene. Abundances of all discoasters, or discoasters at the species level, show only (surprisingly) weak correlations to carbonate contents or oxygen and carbon isotopes of bulk sediment when calculated over the entire sample interval.

Keywords: Miocene, *Discoaster* spp., equatorial Pacific, five major morphogroups, abundance variations

Received 4 December 2015; accepted 18 April 2016

Miocene times were characterized by major changes in ocean circulation and global climate that were driven by a complex set of factors operating on tectonic, orbital and suborbital time scales (Zachos *et al.* 2001). This time-dependent development of Miocene palaeoenvironmental conditions is reflected in the distribution and evolutionary patterns, often expressed in terms of biostratigraphic resolution, among the dominant sediment-forming oceanic plankton groups (Kennett & Srinivasan 1983; Perch-Nielsen 1985; Baldauf & Barron 1990). In a review of Miocene through Pleistocene open-ocean calcareous nannofossil evolutionary appearances and extinctions, Raffi *et al.* (2006) show eight biochronologically useful biohorizons between 23 and 14 Ma, giving an average rate of 1.5 biohorizons per million years. In the next following eight million years (14–6 Ma), the number of biohorizons are 29 (3.6 biohorizons/million years), representing well over a doubling of the rate of taxonomic evolution among open-ocean calcareous nannofossils compared with that of the early half of the Miocene. Nearly half (14 of 29) of Raffi's biohorizons in the younger half of the Miocene are represented by members of the genus *Discoaster*. This key group (genus) among Cenozoic calcareous nannofossils thus demonstrates a distinct evolutionary response to changing conditions in the photic zone of the middle and late Miocene oceans, if assuming that discoasters belonged to the Haptophytes, a specific group of unicellular photosynthetic protists. This assumption is supported by the group's environmental distribution (marine), its abundance (a dominant component of fine-grained low to middle latitude carbonate sediments over a *c.* 55 Ma long time interval [note that we follow Holden *et al.* (2011) in referring to both absolute age and time durations as Ma, in order to achieve 'compliance with the international standard']), size range (4–30 µm), mineralogy (low magnesium calcite) and obvious biological origin. However, fossil *Discoaster*-bearing coccospheres have never been observed.

Discoasters are considered to thrive in warmer waters (Edwards 1968; Perch-Nielsen 1972; Bukry 1973a; Haq & Lohmann 1976), although Wei & Wise (1990) pointed out that there is no simple linear relationship between *Discoaster* abundance and water temperature. Discoasters have been suggested to thrive also under oligotrophic conditions (Chepstow-Lusty *et al.* 1989, 1992; Gibbs *et al.* 2004). This makes the Eastern Equatorial Pacific (EEP) an interesting place for the study of Miocene discoasters, as this region offers equatorial temperatures combined with high nutrient availability and productivity conditions in the photic zone via wind-driven upwelling (Pennington *et al.* 2006). This upwelling system in the EEP appears to have been operational for tens of millions of years (Moore *et al.* 2004).

Higher-resolution stratigraphic studies of Neogene calcareous nannofossils from this environmental setting in the EEP have demonstrated that the distribution of Neogene *Discoaster* taxa exhibits rapid fluctuations in abundance, or even discontinuous occurrences over short stratigraphic intervals (Raffi & Flores 1995; Raffi *et al.* 1995; Backman *et al.* 2013). Furthermore, discoasters are considered to be among the least dissolution-susceptible calcareous nannofossils (Bukry 1971a, 1973a; Roth & Thierstein 1972; Lohmann & Carlson 1981).

The abundance fluctuations, or absence, of discoasters in Neogene carbonate sediments of the EEP are here, therefore, assumed to mainly reflect variable conditions in the sunlit uppermost part of the water column, in which some set of conditions promoted and some other set of conditions suppressed the productivity of discoasters.

Abundance data of *Discoaster* assemblages in Miocene sediments have been generated from IODP Site U1338, located in the EEP at 2° 30.469' N, 117° 58.174' W at a water depth of 4210 m (Pälike *et al.* 2010). This Miocene sediment sequence at Site U1338 may be considered to reflect variations in photic zone conditions

and *Discoaster* productivity during its plate tectonic travel from a position *c.* 76 km south of the Equator at 17–18 Ma to its present location *c.* 278 km north of the Equator. The Equator crossing occurred at about 10 Ma (Pälike *et al.* 2010).

A key aim of the present study is to investigate abundance variations, evolutionary trends and biostratigraphic properties among upper lower Miocene through upper Miocene members of the genus *Discoaster* at IODP Site U1338. Moreover, we investigate possible correlations between *Discoaster* abundance fluctuations and palaeoenvironmental conditions in the mixed layer (photic zone).

Material and methods

The composition of Site U1338 sediments changes from chalks in the upper lower Miocene sequence to oozes in the upper Miocene, with frequent and rapid changes in the proportions between calcareous and biosiliceous components. Non-biogenic components are consistently <5% (Pälike *et al.* 2010).

The interval examined represents a continuous 336 m thick, spliced sequence from three holes of upper lower through uppermost Miocene sediment between 406 and 72 m CCCSF-A. This depth scale refers to metres compressed composite depth. For Site U1338, this scale corresponds to the CCSF-A depth, or metres composite depth in the splice of the three holes drilled at this site, divided by a factor of 1.107 (Pälike *et al.* 2010). Their shipboard splice was subsequently revised by Wilkens *et al.* (2013). This revised splice of Site U1338 is used here, and all depths given below and in plots refer to the revised CCSF-A depth scale of Wilkens *et al.* (2013), divided by 1.107; this compressed CCSF-A scale is referred to as CCSF-B (=CCCSF-A) by Pälike *et al.* (2010, Site U1338, p. 29). Furthermore, depths of *Discoaster* locations are given as mid-points between nearest samples, for example, the base of *Discoaster bellus* occurs between 225.14 m and 225.87 m, giving a mid-point at 225.51 m.

The investigated 336 m thick sediment sequence represents the time interval between *c.* 17.8 and 5.3 Ma, resulting in an average sedimentation rate of *c.* 27 m Ma⁻¹. All age estimates refer to the time scale of Lourens *et al.* (2004).

Magnetostratigraphy exists in two shorter intervals, from 9.098 Ma (top C4Ar.1r) to 9.987 Ma (top C5n.2n), and 12.730 Ma (top C5Ar.1n) to 15.160 Ma (top C5Br), respectively. These two intervals with magnetostratigraphy together encompass <27% of the investigated time interval, implying that age information in the remaining 73% relies on biochronological interpretation of biostratigraphic data. Sedimentation rates based on biochronology commonly imply interpolation between widely separated biohorizons. We have, therefore, chosen to present the abundance data *v.* depth rather than age, as age estimates inevitably will change when an improved age model based on astronomical tuning of various sediment properties becomes established. However, when summarizing relative abundances of the major *Discoaster* groups, we have placed these data on a low-resolution age model for Site U1338 (Backman *et al.* 2016), using a combination of seven biomagnetostratigraphic indicators from 5.04 Ma/68.63 m to 17.74 Ma/406.43 m.

The 494 smear-slides were prepared following the technique of Bown & Young (1998).

Sample distances vary along the studied interval, with an average depth resolution of one (1) sample every 68 cm. Smear-slides were analysed using a light microscope at 1250× magnification. Abundance data were obtained by counting the relative abundance of *Discoaster* species relative to the total number of discoasters, expressed as a percentage, and the number of specimens in a prefixed area on the smear-slide (number of specimens per mm²), following Backman & Shackleton (1983). The calcareous nannofossil biozonation by Backman *et al.* (2012) was employed.

Morphometric analyses were performed using the image analysis software Image-Pro Plus 6.2. The *Discoaster* data presented here are from an unpublished PhD thesis (Ciummelli, M. 2013. *Morphometry, evolution, biostratigraphy and ecology of the genus Discoaster in the Miocene using material from Site U1338, IODP Exp. 321*. Università degli Studi 'G. d'Annunzio', Chieti-Pescara, 1–129).

Author citations for *Discoaster* species discussed below are to be found in Aubry (1984) and Perch-Nielsen (1985).

Taxonomy and abundance behaviour of five major groups of Miocene discoasters at IODP Site U1338

Discoaster assemblages evolved rapidly during late early through late Miocene times, resulting in a series of biohorizons that have proved useful in marine biostratigraphy. Robust morphotypes with broad rays were dominant during the early Miocene. These were successively replaced with more slender, thinner-rayed morphotypes during the middle Miocene, an evolutionary trend that Bukry (1971b) considered to reflect the cooling of the Cenozoic oceans. Following the middle Miocene, discoasters stayed thin-rayed until their extinction at the base of the Olduvai subchron (Backman & Pestiaux 1987). The mutual extinction of the two final *Discoaster* morphotypes, one with six slender rays (*D. brouweri*) and a three-rayed variety (*D. triradiatus*), was first recognized by Takayama (1969), who referred to the latter as '3-rayed *D. brouweri*'.

The Site U1338 Miocene discoasters that are confidently referred to the species level can be brought together into five broad morphological categories based on ray numbers, ray terminations and central area size:

- (1) six-rayed morphotypes with bifurcated ray tips;
- (2) six-rayed morphotypes with large central areas;
- (3) six-rayed morphotypes with pointed ray tips;
- (4) five-rayed morphotypes with bifurcated ray tips;
- (5) five-rayed morphotypes with pointed ray tips.

Six-rayed morphotypes with bifurcated ray tips

A group of six-rayed discoasters with bifurcated ray tips includes both thicker- and thinner-rayed morphotypes (Fig. 1:1–1:20). A robust structure with thicker-rayed morphotypes characterizes the following species: *D. deflandrei*, *D. aulakos*, *D. divaricatus*, *D. woodringi* and *D. icarus*. These are hereafter informally referred to as the *D. deflandrei* group (Fig. 1:1–1:5, 1:12). A more slender ray structure characterizes *D. variabilis*, *D. exilis*, *D. cf. exilis*, *D. signus*, *D. cf. signus*, *D. cf. bollii*, *D. surculus* and *D. loeblichii*. These are hereafter informally referred to as the *D. variabilis* group (Fig. 1:6–1:11, 1:14–1:16). Forms with intergrading morphologies between *D. variabilis* and *D. exilis* on the one hand, and *D. variabilis* and *D. icarus* on the other, are also included in the *D. variabilis* group.

The Discoaster deflandrei group

The species included in this group are characterized by six thick bifurcated rays that radiate symmetrically from a well-developed central area. The angle between the bifurcations varies, and so do their shape, from angular to rounded. These characters have been used to distinguish similar-looking species (Gartner 1967; Hay *et al.* 1967; Aubry 1984).

Two additional species have been referred to the *D. deflandrei* group, namely *D. saundersi* (Hay *et al.* 1967) and *D. tinquarensis* (Furrazzola-Bermúdez & Itturalde 1967). In this study, only *D. aulakos*, *D. divaricatus* and *D. woodringi* were observed (Fig. 1:3–1:5). The latter species was described by Bramlette & Riedel (1954) and has been considered to represent an artificial species

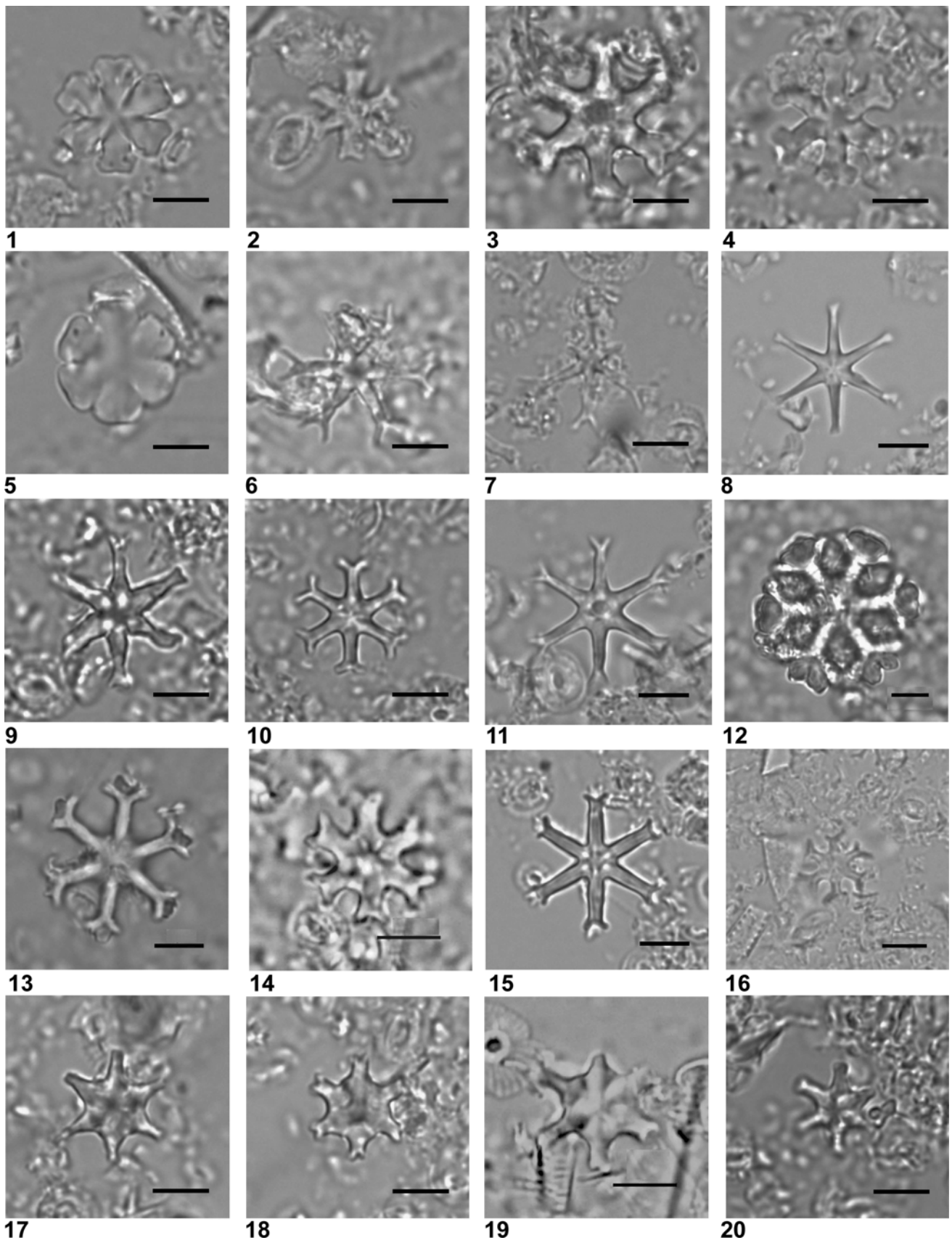


Fig. 1. 1, *Discoaster deflandrei* (sample U1338C-46H-2, 45–46 cm). 2, Intergrading form *Discoaster deflandrei*–*Discoaster variabilis* (sample U1338C-31H-3, 122–123 cm). 3, *Discoaster aulakos* (sample U1338B-26H-5, 120–121 cm). 4, *Discoaster divaricatus* (sample U1338C-44H-2, 120–121 cm). 5, *Discoaster woodringi* (sample U1338C-46H-5, 45–46 cm). 6, *Discoaster signus* (sample U1338C-39H-2, 122–123 cm). 7, *Discoaster* cf. *signus* (sample U1338C-41H-6, 44–45 cm). 8, *Discoaster exilis* (sample U1338A-25H-2, 80–81 cm). 9, *Discoaster* cf. *exilis* (sample U1338B-42H-4, 45–46 cm). 10, *Discoaster variabilis* (sample U1338B-18H-4, 45–46 cm). 11, Intergrading form *Discoaster variabilis*–*Discoaster exilis* (sample U1338A-25H-3, 80–81 cm). 12, *Discoaster icarus* (sample U1338B-18H-6, 120–121 cm). 13, Intergrading form *Discoaster variabilis*–*Discoaster icarus* (sample U1338B-16H-3, 120–121 cm). 14, *Discoaster* cf. *bollii* (sample U1338A-24H-4, 58–59 cm). 15, *Discoaster surculus* (sample U1338A-24H, CC). 16, *Discoaster loeblichii* (sample U1338A-18H-6, 45–46 cm). 17–18, *Discoaster kugleri* (sample U1338B-28H-6, 45–46 cm). 19–20, *Discoaster musicus* (19 – sample U1338A-25H-4, 120–121 cm; 20 – sample U1338B-33H-5, 45–46 cm). Scale bar 5 μ m.

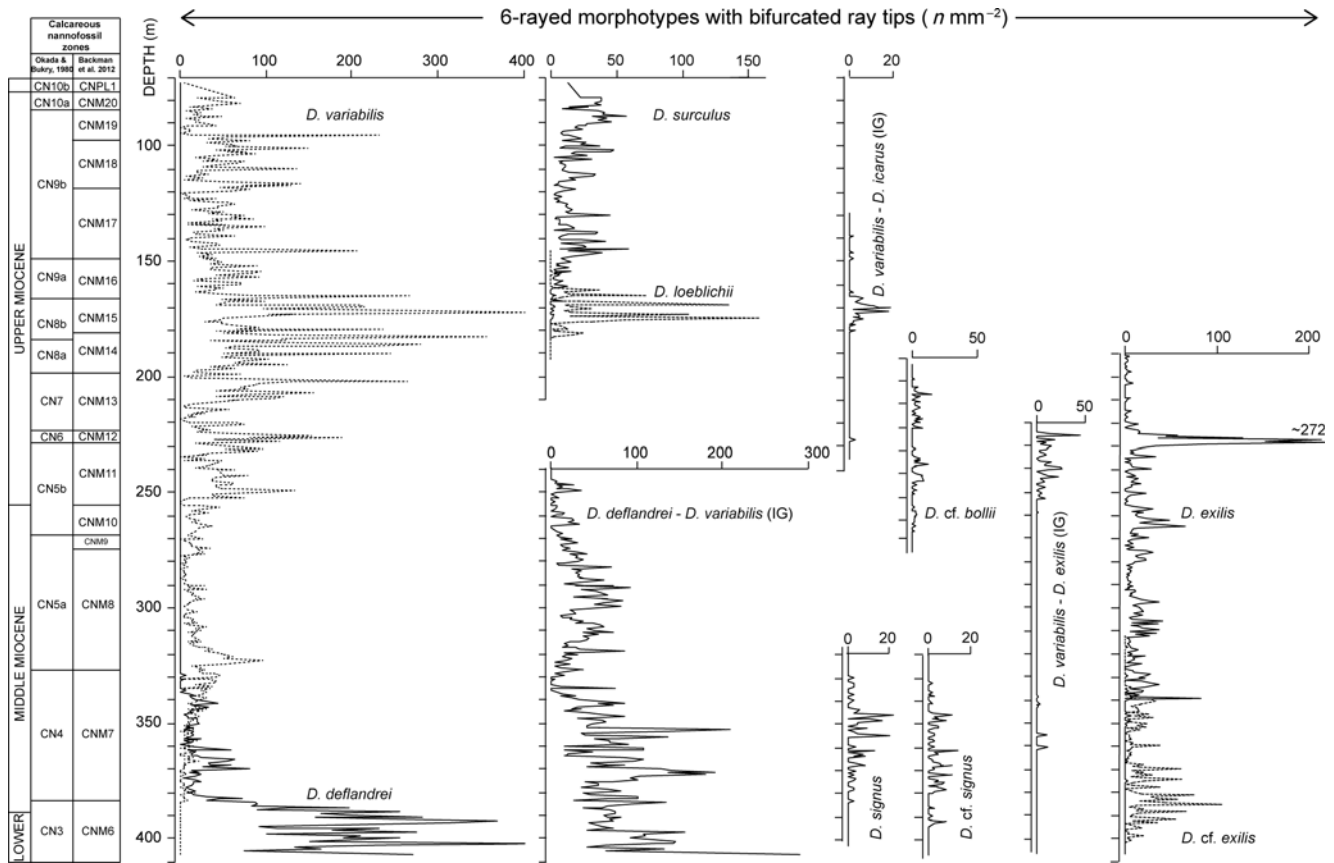


Fig. 2. Abundance data as number of specimens of six-rayed discoasters having bifurcated ray tips in a prefixed area on the smear-slide at Site U1338. Biozonations from Okada & Bukry (1980) and Backman *et al.* (2012). Depth refers to compressed metres composited depth (see ‘Methods’ section). (IG) denotes specimens showing intergrading morphology between two species.

whose morphology is created by secondary calcite overgrowth (Roth & Thierstein 1972; Aubry 1984; Rio *et al.* 1990). This view is supported by our observations from Site U1338, where *D. woodringi* morphotypes occur in the lowermost part of the sequence where the preservation of nannofossil assemblages is deteriorated by calcite overgrowth and/or dissolution.

Discoaster aulakos and *D. divaricatus* (Fig. 1:3–1:4) were observed in middle Miocene sediments at Site U1338. Aubry (1984) described in detail the differences between these species. In

the census data from Site U1338, however, we grouped these similar-looking morphotypes in the broader *D. deflandrei* concept, thus avoiding splitting the group on the basis of preservational biases caused by overgrowth and/or dissolution, and allowing for some degree of intra-specific morphological variation of *D. deflandrei*. This grouping was made despite the fact that some specimens referable to the *D. aulakos* and *D. divaricatus* concepts were observed. Many other specimens, however, could not be properly separated from *D. deflandrei*. Furthermore, *D. aulakos* and

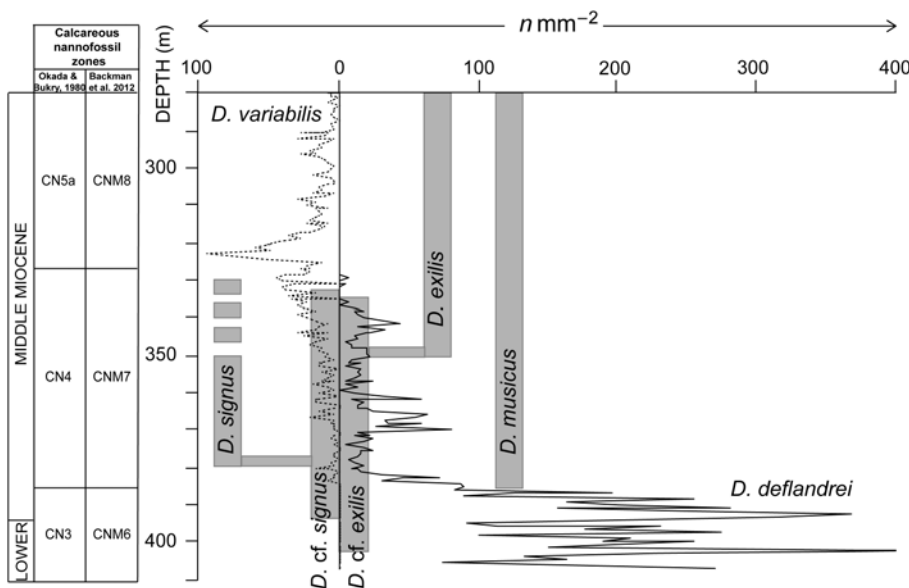


Fig. 3. Sequence of *Discoaster* evolutionary events across the early/middle Miocene boundary at Site U1338, together with abundance data of *D. deflandrei* and *D. variabilis*. These changes represent the first major evolutionary transition among Miocene discoasters. Biozonations from Okada & Bukry (1980) and Backman *et al.* (2012). Depth refers to compressed metres composited depth (see ‘Methods’ section). These changes represent the first major evolutionary transition among Miocene discoasters.

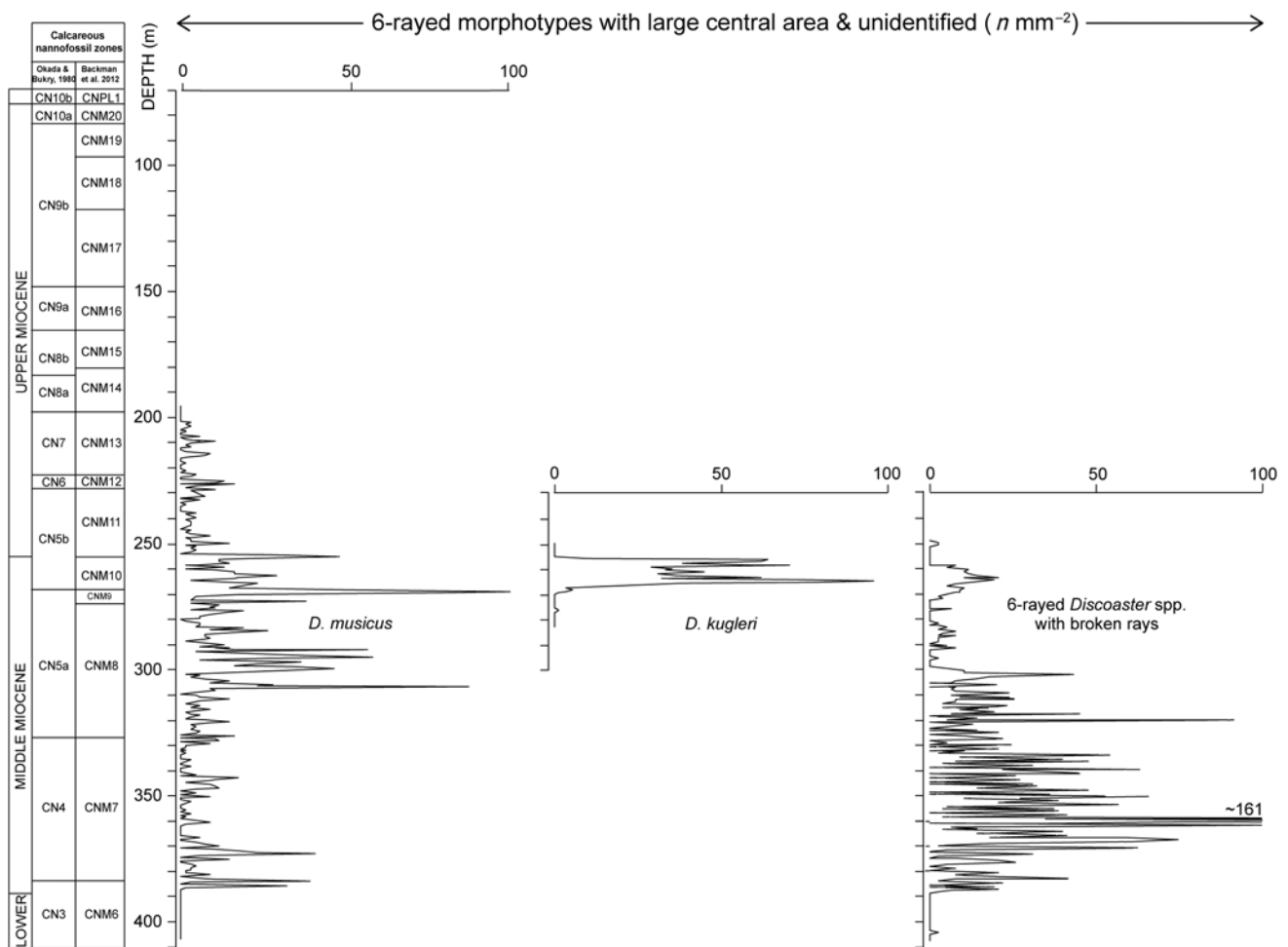


Fig. 4. Abundance data as number of specimens of six-rayed discoasters having large central areas in a prefixed area on the smear-slide at Site U1338. Biozonations from Okada & Bukry (1980) and Backman *et al.* (2012). Depth refers to compressed metres composited depth (see ‘Methods’ section).

D. saundersi have been considered to represent ‘an intermediate variety between *D. deflandrei* and *D. exilis*’ by Jeremy Young (16 March 2011, nannotax.org), who also considers both *D. divaricatus* and *D. saundersi* to be synonyms of *D. deflandrei*.

Bukry (1973b, p. 692) noticed that

[a] reduction in the dominance of *Discoaster deflandrei* at the top of the zone [*H. ampliapertura* Zone] in favor of long-rayed discoasters such as *D. exilis*, *D. signus*, and *D. variabilis* is distinctive in low-latitude areas

and referred to this as an ‘end of Acme’ of *D. deflandrei* without quantifying the concept. Subsequently, Rio *et al.* (1990) quantified this biohorizon as when the abundance of *D. deflandrei* decreased to values below 30% among the total *Discoaster* assemblage, and remarked that this event coincides with the appearance of *D. signus*. These changes occur also at Site U1338, together with the appearances of *D. variabilis* and morphotypes here referred to as *D. cf. exilis* (Figs 2 and 3).

The exact position of the *D. deflandrei* decline, however, is obscured at Site U1338 because of poor preservation among many specimens that belong to the *D. deflandrei*/*D. variabilis* plexus together with presence of morphotypes showing intergrading morphologies between the two morphotype end-members (Fig. 2). This makes it difficult to apply the 30% rule if taking into account also poorly preserved and intergrading forms (*D. deflandrei*–*D. variabilis* (IG) in Fig. 2) in the lowermost part of the investigated sequence at Site U1338. However, if taking into

account only specimens that have been identified with certainty as *D. deflandrei*, the 30% limit distinctly falls between 384.92 and 385.60 m (Fig. 2).

Discoaster icarus (Fig. 1:12) is another robust six-rayed form that shows morphological similarities with ‘species’ in the *D. deflandrei* group. This morphotype is separated, however, from the *D. deflandrei* group in terms of its restricted stratigraphic distribution in sediments of Messinian age (Stradner 1973). *Discoaster icarus* thus appeared about eight million years after the top of common *D. deflandrei* in the lowermost middle Miocene (Backman *et al.* 2013). *Discoaster icarus* is a large, up to 30 μm , morphotype characterized by its large central area bearing a hexagonal or prismatic knob on the distal side and sutures on both the distal and proximal sides. The sutures delineate the roots of six robust rays ending in wide-angled bifurcations and presence of a membrane-like structure between them (Stradner 1973; Aubry 1984). This morphotype is rare at Site U1338, whereas specimens showing intermediate morphologies with *D. variabilis* (Fig. 1:13) are more common (Fig. 2).

The *Discoaster variabilis* group

Discoaster variabilis was originally described by Martini & Bramlette (1963), a species characterized by long and slender rays that may bend slightly, and having bifurcating ray tips. The *D. variabilis* concept refers to discoasters with a large degree of morphological variability due to differences in ray numbers (3–6), ray terminations and central area sizes. The bifurcations can be more or less developed and sometimes show a web between them (Aubry 1984). This is evident in the sporadic occurrences of intermediate

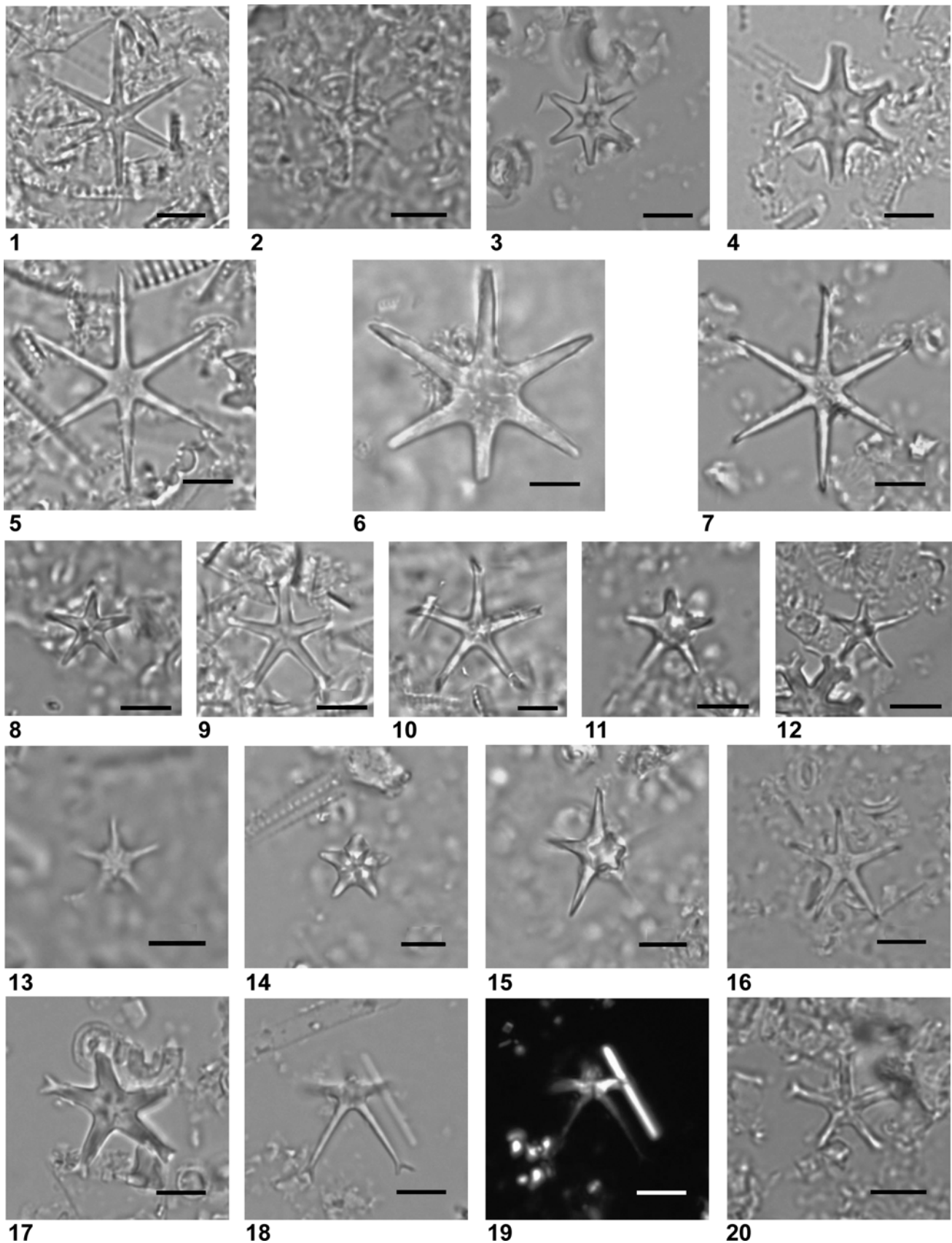


Fig. 5. **1**, *Discoaster brouweri* (sample U1338A-13H-3, 120–121 cm). **2**, *Discoaster* cf. *brouweri* (sample U1338C-31H-3, 122–123 cm). **3**, *Discoaster intercalaris* (sample U1338A-22H-5, 80–81 cm). **4**, Intergrading form *Discoaster variabilis*–*Discoaster intercalaris* (sample U1338A-19H-5, 45–46 cm). **5**, *Discoaster brouweri* >20 μm (sample U1338A-13H-3, 120–121 cm). **6**, *Discoaster neorectus* (sample U1338A-18H-5, 120–121 cm). **7**, *Discoaster neohamatus* (sample U1338B-13H-2, 120–121 cm). **8**, *Discoaster bellus* (sample U1338B-18H-5, 120–121 cm). **9**, Intergrading form *Discoaster bellus*–*Discoaster hamatus* (sample U1338B-24H-3, 142–143 cm). **10**, *Discoaster hamatus* (sample U188A-24H-2, 68–69 cm). **11–12**, Intergrading form *Discoaster bellus*–*Discoaster berggrenii* (11 – sample U1338B-18H-5, 120–121 cm; 12 – sample U1338B-18H-4, 45–46 cm). **13–14**, *Discoaster berggrenii* (13 – sample U133A-18H-6, 45–46 cm; 14 – sample U1338B-13H-2, 120–121 cm). **15**, *Discoaster quinqueramus* (sample U1338B-13H-2, 120–121 cm). **16**, *Discoaster asymmetricus* (sample U1338A-16H-3, 45–46 cm). **17**, *Discoaster moorei* (sample U1338A-25H-3, 80–81 cm). **18–19**, *Discoaster pentaradiatus* (sample U1338A-9H-5, 70–71 cm). **20**, *Discoaster prepentaradiatus* (sample U1338A-21H-2, 66–67 cm). Scale bar 5 μm .

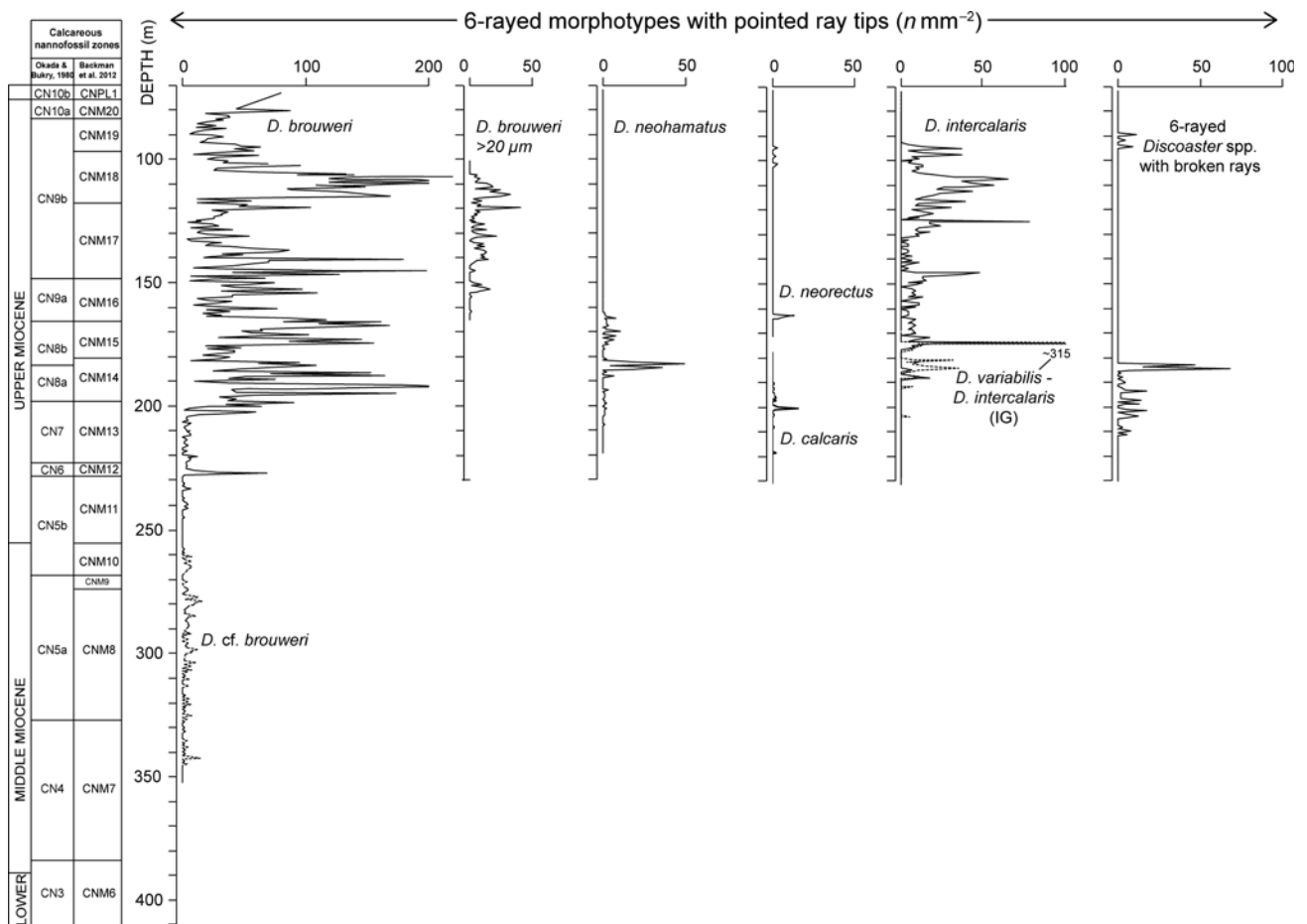


Fig. 6. Abundance data as number of specimens of six-rayed discoasters having pointed ray tips in a prefixed area on the smear-slide at Site U1338. The rapid rise of *D. brouweri* close to 200 m is a key part of the second major evolutionary transition among Miocene discoasters (see also Figs 10 and 11). Biozonations from Okada & Bukry (1980) and Backman *et al.* (2012). Depth refers to compressed metres composited depth (see ‘Methods’ section). (IG) denotes specimens showing intergrading morphology between two species. Notice 16 m stratigraphic gap between the disappearance of *D. cf. brouweri* and appearance of *D. brouweri*. Plot modified from Backman *et al.* (2013).

specimens between *D. variabilis* and *D. icarus*, recorded in a restricted stratigraphic interval from 227.40 to 138.81 m (Figs 1:13, 2). Intermediate specimens between *D. variabilis* and *D. exilis* also exist (Figs 1:11, 2). These differences have resulted in descriptions of several species that are here informally referred to the *D. variabilis* group. Examples include *D. challengerii*, described by Bramlette & Riedel (1954), and *Discoaster variabilis pansus*, described by Bukry & Percival (1971). In their discussion of this sub-species, Bukry & Percival informally referred to the ‘main stock’ of *D. variabilis* as *D. variabilis variabilis*.

It seems plausible that the phenomenon of hybridization involves *D. variabilis* and other discoasters like *D. exilis* and *D. intercalaris*. The central area is well developed and in the convex side a stellate knob is present while, in the concave side, small ridges run out from the central knob along the median line of each ray (Aubry 1984). Young (1998) suggests that *D. variabilis* evolved from *D. exilis* during the early late Miocene while Prins (1971) and Theodoridis (1984) argue that *D. variabilis* evolved from *D. deflandrei*.

Discoaster exilis was described by Martini & Bramlette (1963) and has six long rays with bifurcated tips. At Site U1338, this species was occasionally difficult to recognize due to calcite overgrowth. Specimens referred to as *D. cf. exilis* (Fig. 1:9) are recorded from below and into the range of typical *D. exilis* (Figs 1:8, 2) and overlap with the uppermost range of members belonging to the *D. deflandrei* group. Specimens of *D. cf. exilis* differ from *D. exilis* in lacking the typical ridges along the rays. Intermediate forms between *D. variabilis* and *D. exilis* are common,

having an overall structure similar to that of *D. variabilis* and the bifurcated terminations of *D. exilis*.

Discoaster signus is characterized by thin bifurcated terminations and a prominent knob in the central area. Moshkovitz & Ehrlich (1980) and Filewicz (1985) described two species, *Discoaster petaliformis* and *Discoaster tuberi*, respectively, that Backman *et al.* (2012) consider to be junior synonyms of *D. signus*. Specimens similar to *D. signus* were observed below and throughout the range of typical *D. signus* (Figs 1:6, 2). These morphotypes, referred to as *D. cf. signus*, have small and thin bifurcations and an outline similar to that of *D. signus* but lack the typical star-shaped central knob (Fig. 1:7) and are here considered to represent intermediate forms between *D. signus* and *D. exilis*.

According to the abundance data from Site U1338, there appears to be an evolutionary step-like succession from *D. deflandrei* to *D. variabilis* to *D. signus* to *D. exilis* (Fig. 3). The major decrease in *D. deflandrei* near 385 m occurs together with the first occurrence of typical *D. variabilis*, closely followed by the first typical *D. signus*. The final step is the occurrence of the first typical *D. exilis* together with the final occurrence of typical *D. deflandrei*. This suggests that *D. deflandrei* may be the ancestor of *D. variabilis* as well as *D. signus* and *D. exilis*. The roles of *D. cf. signus* and *D. cf. exilis* in this evolutionary succession are unclear, partly because preservational problems are involved in our designation of these morphotypes and partly because genuine evolutionary transitions cannot be excluded; these morphotypes may represent ‘precursors’ of the typical *D. signus* and *D. exilis*.

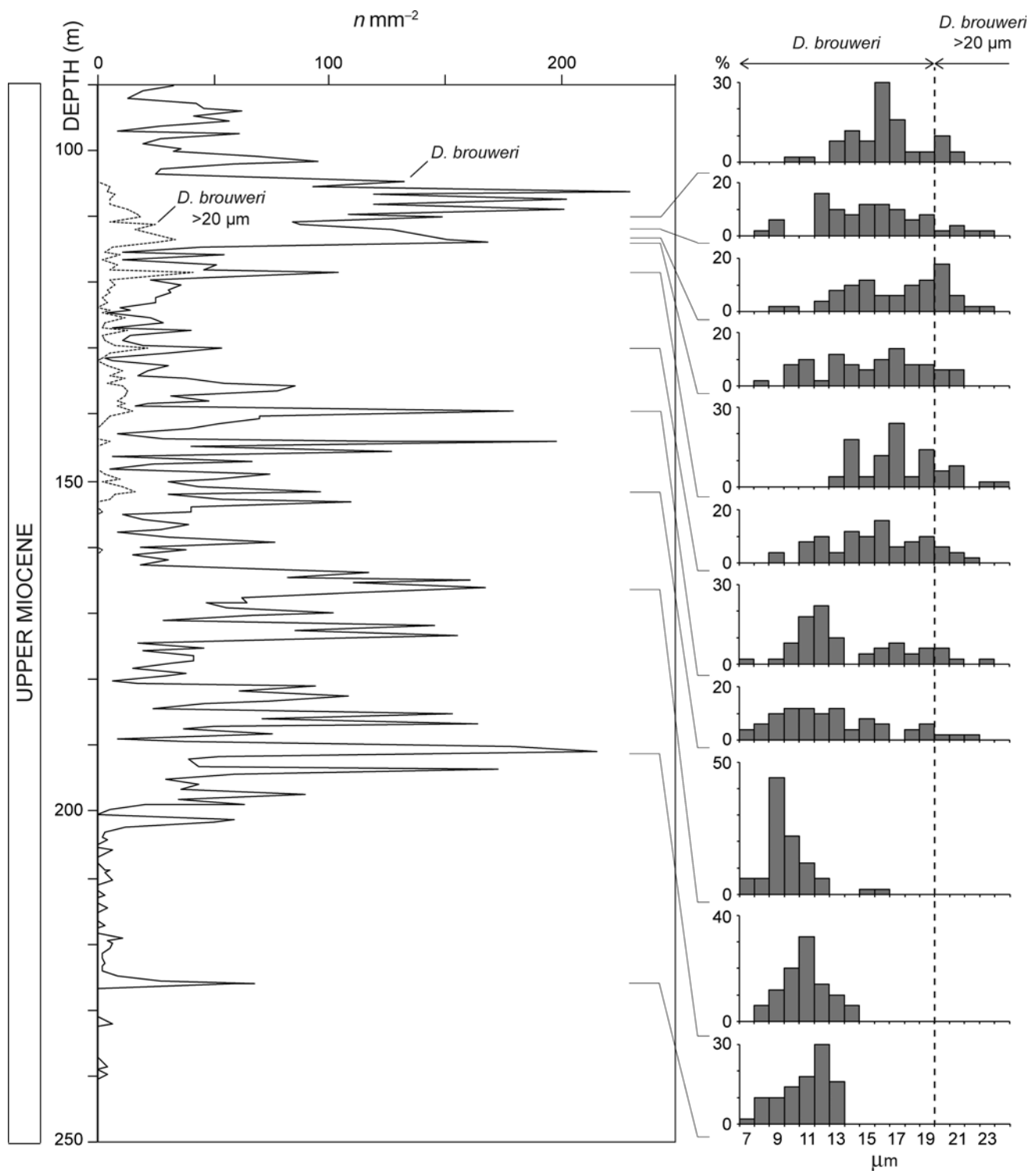


Fig. 7. Abundances and biometry of *D. brouweri* in the late Miocene, revealing a nearly 50% size increase, on average. Specimens $>20\ \mu\text{m}$ are plotted separately in the abundance plot, following the *Discoaster* sp. 2 concept of Rio *et al.* (1990) and Raffi *et al.* (1995). Histograms represent relative abundances (%) using $1\ \mu\text{m}$ size increments. Data were acquired using the image analysis software Image-Pro Plus 6.2.

Typical *Discoaster bollii*, characterized by short tapering, bifurcated rays and a distinct central knob, have not been observed at Site U1338. Rare specimens approaching the morphology of *D. bollii* were, however, observed (Fig. 1:14), referred to as *D. cf. bollii*.

Discoaster surculus and *D. loeblichii* represent two species with six slender and bifurcated rays observed at Site U1338 (Fig. 1:15–1:16). Bukry (1973b) suggested that *D. surculus* may have evolved from *D. pseudovariabilis*, a species not observed at Site U1338. *Discoaster loeblichii* is well preserved at Site U1338

with specimens having the typical asymmetrical bifurcation of the ray tips.

In the middle Miocene sediments at Site U1338, the abundance of other six-rayed discoasters having bifurcated ray tips which could not be confidently referred to either the *D. deflandrei* group or the *D. variabilis* group because of overgrowth problems or intergrading morphologies have been counted separately (Fig. 2). These specimens are here referred to as *D. deflandrei*–*D. variabilis* intergrading (IG) morphotypes (Fig. 1:2). In this middle Miocene interval, poorly preserved six-rayed discoasters are present, having

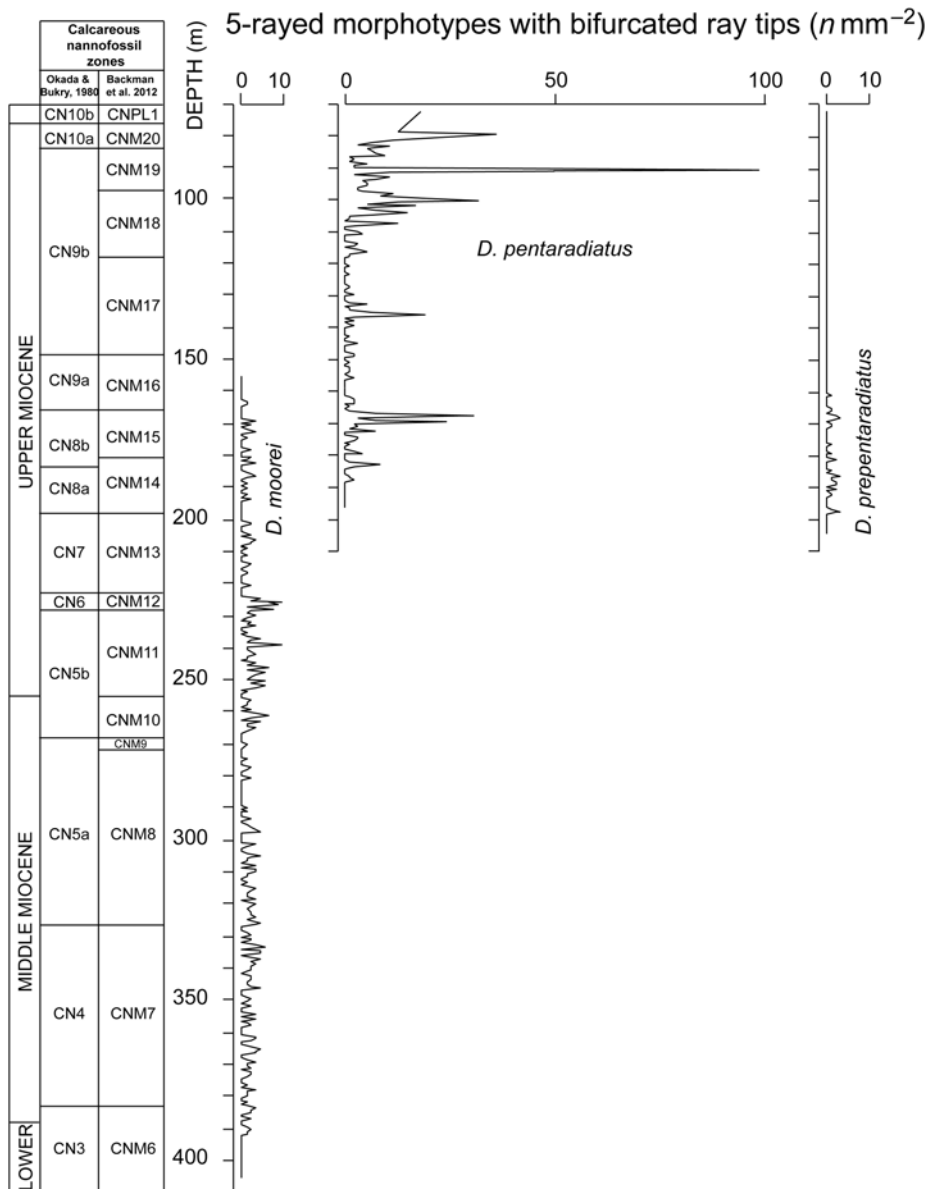


Fig. 8. Abundance data as number of specimens of five-rayed discoasters having bifurcated ray tips in a prefixed area on the smear-slide at Site U1338. Biozonations from Okada & Bukry (1980) and Backman *et al.* (2012). Depth refers to compressed metres composited depth (see ‘Methods’ section).

the outer portion of one or several rays broken off, referred to as ‘6-rayed *Discoaster* spp. with broken rays’. These may represent *D. deflandrei*, *D. deflandrei*–*D. variabilis* (IG), *D. variabilis*, *D. signus*, *D. cf. signus*, *D. exilis* or *D. cf. exilis*.

Six-rayed morphotypes with a large central area

A group of six-rayed discoasters characterized by a large central area includes the middle Miocene species *D. musicus*, *D. sanmiguelensis* and *D. kugleri* (Fig. 1:17–1:20). *Discoaster musicus* and *D. sanmiguelensis* were described by Stradner (1959) and Bukry (1981), respectively, using similar diagnostic characters. A comparison of Stradner’s and Bukry’s descriptions and illustrations suggests that *D. sanmiguelensis* is a junior synonym of *D. musicus*, as suggested previously by Rio *et al.* (1990). These morphotypes are here merged under the *D. musicus* concept (Fig. 4) as it was not possible to consistently separate the two, particularly when calcite overgrowth blurred morphological features. The first appearance of *D. musicus* at Site U1338 occurs concomitantly with the sharp decrease in abundance of *D. deflandrei*, near 385 m (Figs 2–4).

The decline in abundance of *D. deflandrei* at *c.* 385 m in Site U1338 is characterized by an interval of low abundances prior to its extinction, which may be placed at between 336 and 327 m, marking the end of a successful species that had thrived and

dominated the *Discoaster* assemblages over much of its range, encompassing *c.* 30 Ma. Several new species of bifurcated six-rayed discoasters evolved in the *c.* 50 m long stratigraphic interval above the sharp abundance decline of *D. deflandrei*, including *D. musicus*, *D. variabilis*, *D. signus*, *D. exilis* and the pre-cursor morphotypes *D. cf. signus* and *D. cf. exilis* (Figs 2–4). These changes represent the first of two major evolutionary transitions among Miocene discoasters. The precise phylogenetic relationships among these taxa, that share some morphological characters, and their relationship to *D. deflandrei*, cannot be resolved with the available data from Site U1338, partly due to preservational problems. The most logical ancestor for this development among the six-rayed bifurcated discoasters close to the early/middle Miocene boundary is here considered to be *D. deflandrei*. It is noteworthy that the evolution among the 6-rayed bifurcated discoasters began during the later part of the middle Miocene climate optimum (end of dominance of *D. deflandrei*, appearance of *D. variabilis*) and ended (extinction of *D. deflandrei*, appearance of *D. exilis sensu stricto*) when extensive ice growth began on Antarctica (Holbourn *et al.* 2014). They demonstrate, using carbon and oxygen isotope data from Site U1338, that this critical interval was characterized by ‘high-amplitude climate variations, marked by intense perturbations of the carbon cycle’ (Holbourn *et al.* 2014, pp. 21–22) The combination of marked palaeoclimate variability with major

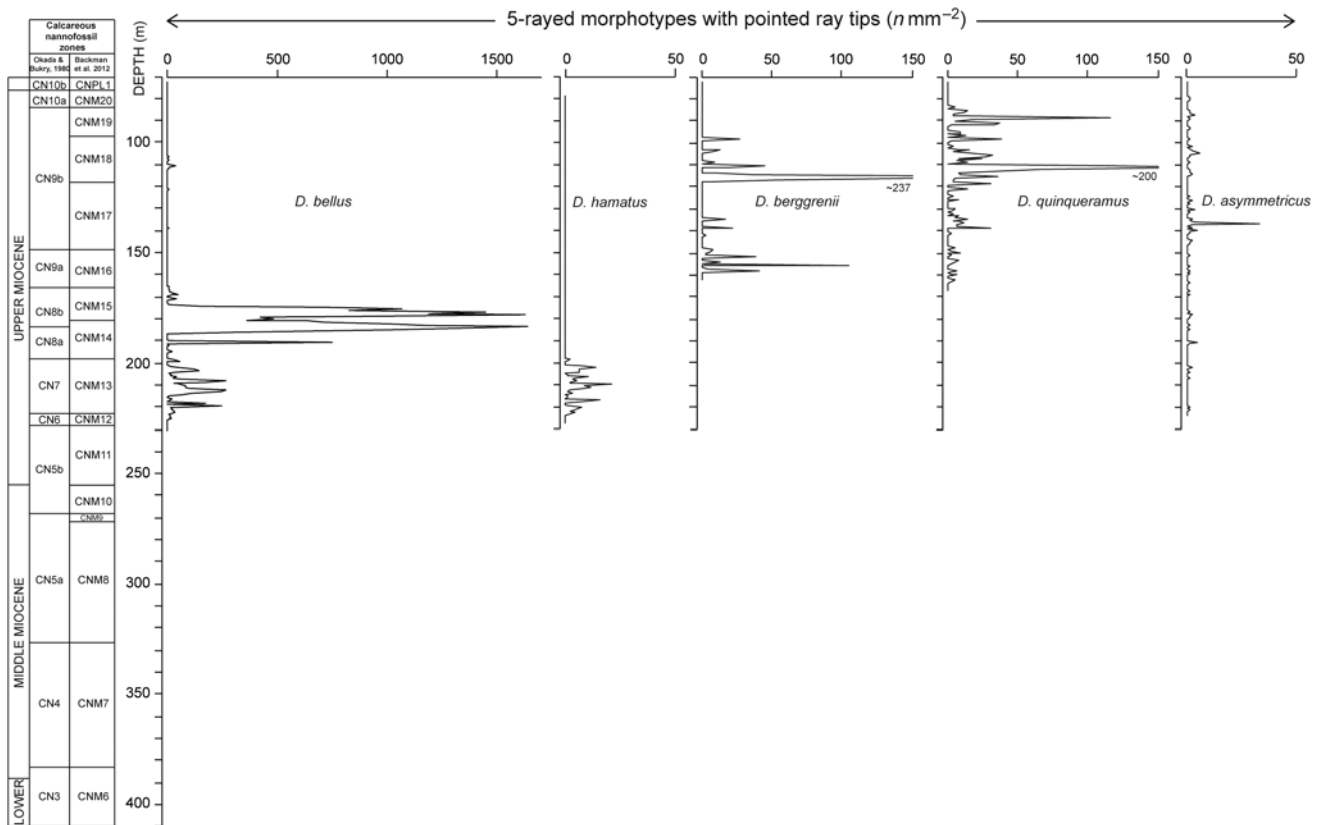


Fig. 9. Abundance data as number of specimens of five-rayed discoasters having pointed ray tips in a prefixed area on the smear-slide at Site U1338. Biozonations from Okada & Bukry (1980) and Backman *et al.* (2012). Depth refers to compressed metres composited depth (see ‘Methods’ section).

biogeochemical changes in the photic zone environments may very well have initiated the major diversification among the middle Miocene *Discoaster* assemblages.

The species *D. kugleri* exhibits differences in terms of lengths and widths of the rays, the bifurcations of ray tips, and in the size of the central area that may or may not show a central knob or sutures. This species shows high abundances across its short total stratigraphic range at Site U1338 (Fig. 4), defining Zone CNM10.

Six-rayed morphotypes with pointed ray tips

A group of six-rayed discoasters with pointed ray tips includes *D. brouweri*, *D. cf. brouweri*, large morphotype (>20 µm) of *D. brouweri*, *D. calcaris*, *Discoaster intercalaris*, *D. intercalaris*–*D. variabilis* (IG), *D. neohamatus* and *D. neorectus* (Fig. 5:1–5:7).

Discoaster brouweri has a simple structure, with six, slightly bent, pointed slender rays. The central area is generally small and lacks ornamentation. In larger specimens, the central area may be more developed as well as the arms, resulting in a more massive morphovariant, similar to *Discoaster neorectus*, which differs from *D. brouweri* by not having umbrella-like bent rays (Bukry 1971a). This similarity between larger *D. brouweri* and *D. neorectus* may indicate an evolutionary link between the two species. Specimens of *D. brouweri* having slender and long rays may resemble *Discoaster neohamatus*. Rio *et al.* (1990, p. 211) suggested that this diagnostic ‘feature is less evident in the specimens found in the terminal range of the species, when intergrade forms to *D. brouweri* are present’.

Discoaster brouweri is common in upper Miocene sediments at Site U1338 (Figs 5:1, 6). Specimens tentatively referred to as ‘*D. cf. brouweri*’ are smaller than typical *D. brouweri* and lack the typical umbrella-like bending of the rays (Fig. 5:2). These smaller forms were observed in low and discontinuous numbers in the middle Miocene (Fig. 6) as low as Zone CNM7, in agreement with the observation by Rio *et al.* (1990) from the tropical Indian Ocean. At

Site U1338, there is a gap in the range between this morphovariant and typical *D. brouweri*.

A large (>20 µm) variety of *D. brouweri* (Fig. 5:5) occurs in the Messinian part of the Miocene at Site U1338. This variety begins at *c.* 155 m (Zone CNM16) and continues to *c.* 105 m (Zone CNM18), within the range of typical *D. brouweri* (Fig. 6). Like *D. brouweri*, this morphovariant is also characterized by a small central area and has been referred to as *Discoaster* sp. 2 by Rio *et al.* (1990), who observed a size range from 20 to 30 µm, from ODP Sites 709–711 in the tropical Indian Ocean. This size range of *Discoaster* sp. 2 has been reported also from ODP Sites 845 and 848 in the eastern equatorial Pacific (Raffi *et al.* 1995). Here, we follow Rio *et al.* (1990) and have plotted forms >20 µm separately (Figs 6 and 7).

Biometric data from image analysis of *D. brouweri* and the large (>20 µm) morphovariant are presented in Figure 7, showing that there is no size gap or bimodal size distribution in the transition from the smaller *D. brouweri* specimens to the larger (>20 µm) morphotype. We notice that between 225 and 166 m, nearly all *D. brouweri* specimens are <14 µm, whereas in the five samples above 130 m nearly all specimens are >12 µm (Fig. 7), marking a distinct increase in size among the *D. brouweri* population during late Miocene times from an average of nearly 11 µm in the late early Miocene to an average of slightly over 16 µm in the late late Miocene. This corresponds to a 49% size increase through the late Miocene.

Obviously, much more biometric data from multiple sites and environmental settings are needed to acquire a more thorough understanding of the relationship between *D. brouweri* and the large morphotype. The appearance of the latter consistently occurs in Zone CNM16 (CN9a) in the low latitude Indian and Pacific oceans (Rio *et al.* 1990; Raffi *et al.* 1995; this study), pointing potentially to a useful lower latitude biostratigraphic marker subdividing the interval between base *Discoaster berggrenii* and base *Amaurolithus primus*.

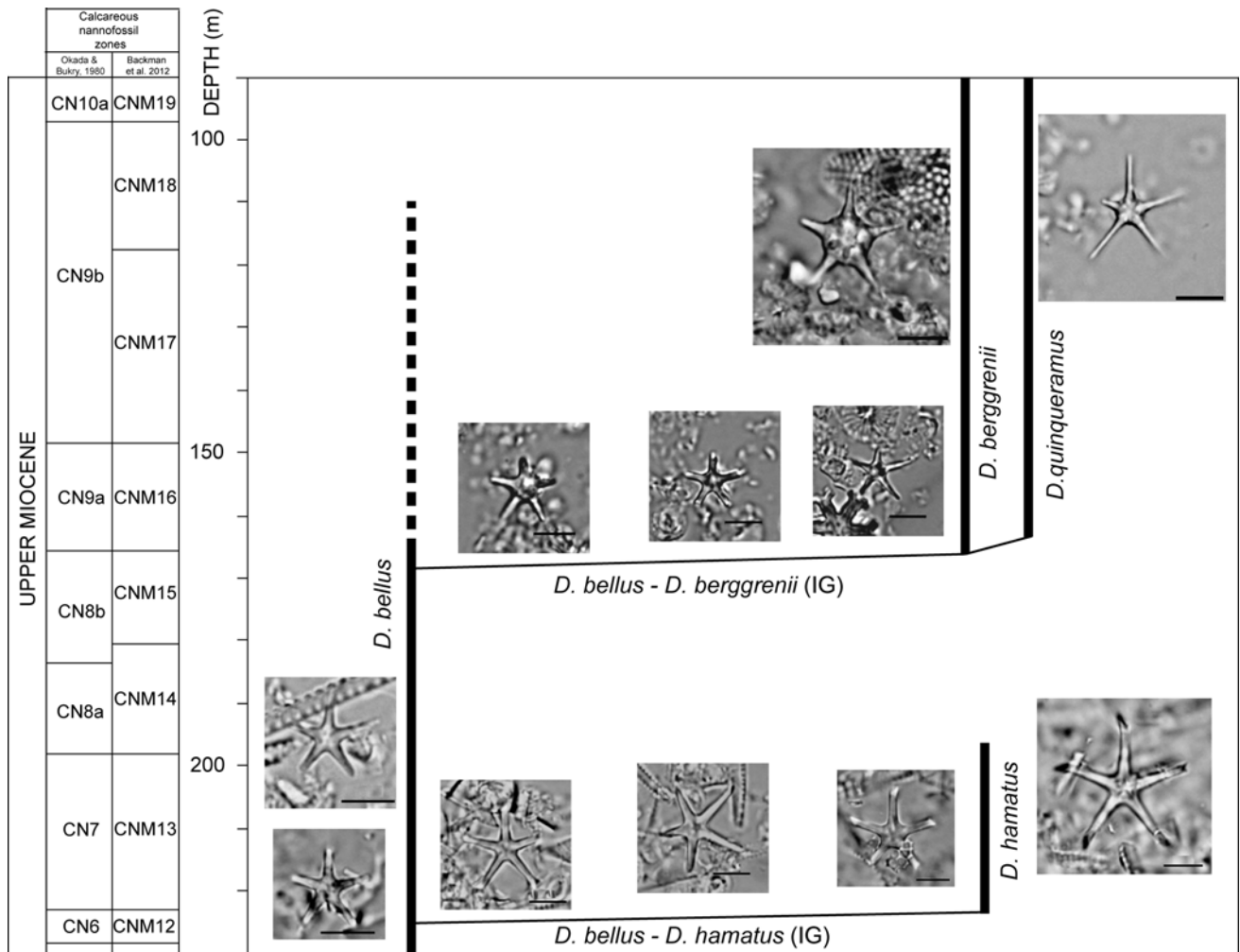


Fig. 10. Successive evolutionary transitions from, first, *D. bellus* to *D. hamatus* and, second, from *D. bellus* to *D. berggrenii*/*D. quinqueramus*. These changes are a key part of the second major evolutionary transition among Miocene discoasters (see also Figs 6 and 11). Biozonations from Okada & Bukry (1980) and Backman *et al.* (2012). Depth refers to compressed metres composited depth (see ‘Methods’ section).

The six slender rays of *D. neohamatus* are long and delicate and extend from a small and featureless central area (Fig. 5:7). At Site U1338, specimens often show broken or partially dissolved rays, which made accurate identifications at the species level difficult. The category ‘6-rayed *Discoaster* spp. with broken rays’ in an interval preceding the presence of typical *D. neohamatus* (Fig. 6) is most probably poorly preserved specimens of *D. neohamatus* with broken ray terminations.

The large (>20 µm) *D. neorectus* is characterized by long straight rays symmetrically arranged with simple tapering tips (Fig. 5:6). *Discoaster neorectus* occurs discontinuously in low numbers in only six samples at Site U1338 (Fig. 6), similar to what has been observed from the tropical Indian Ocean and the eastern equatorial Pacific Ocean (Rio *et al.* 1990; Raffi & Flores 1995). This species consistently overlaps in range with similar-looking large morphotypes of *D. brouweri*, which may suggest an evolutionary relationship between the two. *Discoaster calcaris* also occurs discontinuously in low numbers in 12 samples (Fig. 6).

Discoaster intercalaris shows much morphological variability, ranging in size from 10 to 16 µm and with variable shapes and sizes of the central area and rays, more or less tapering (Fig. 5:3). Intermediate forms with *D. variabilis*, with ray terminations showing a hint of bifurcation, were observed in the lowermost part of its range at Site U1338 (Fig. 5:4). The abundance distributions of these morphotypes are presented in Figure 6.

Five-rayed morphotypes with bifurcating ray tips

A group of five-rayed discoasters with bifurcating ray tips includes *D. moorei*, *D. pentaradiatus* and *D. prepentaradiatus* (Fig. 5:17–5:20). The asymmetrical *D. moorei*, described by Bukry (1971b), has been counted as a separate species (Figs 5:17, 8).

Both birefringent and non-birefringent morphotypes are here included in *D. pentaradiatus*, thereby avoiding the use of the (*Eu-*) *discoaster misconceptus* concept, introduced by Theodoridis (1984) to distinguish slightly birefringent morphotypes. The slight birefringence is useful for recognition of *D. pentaradiatus* because the ray terminations, with thin and fragile bifurcations, are often broken (Fig. 5:18–5:19). *Discoaster prepentaradiatus* differs from *D. pentaradiatus* by having a more robust ray structure and lack of the concave–convex ray shape typical of *D. pentaradiatus* (Fig. 5:20). Both *D. prepentaradiatus* and *D. pentaradiatus* show rare and discontinuous occurrences at Site U1338, although the latter may show single sample peaks of higher abundances (Fig. 8).

Five-rayed morphotypes with pointed ray tips

If the first major evolutionary transition among middle–upper Miocene discoasters was the demise of the *D. deflandrei* group and the emergence of the *D. variabilis* group, the second major transition is the emergence of five-rayed morphotypes with pointed ray tips.

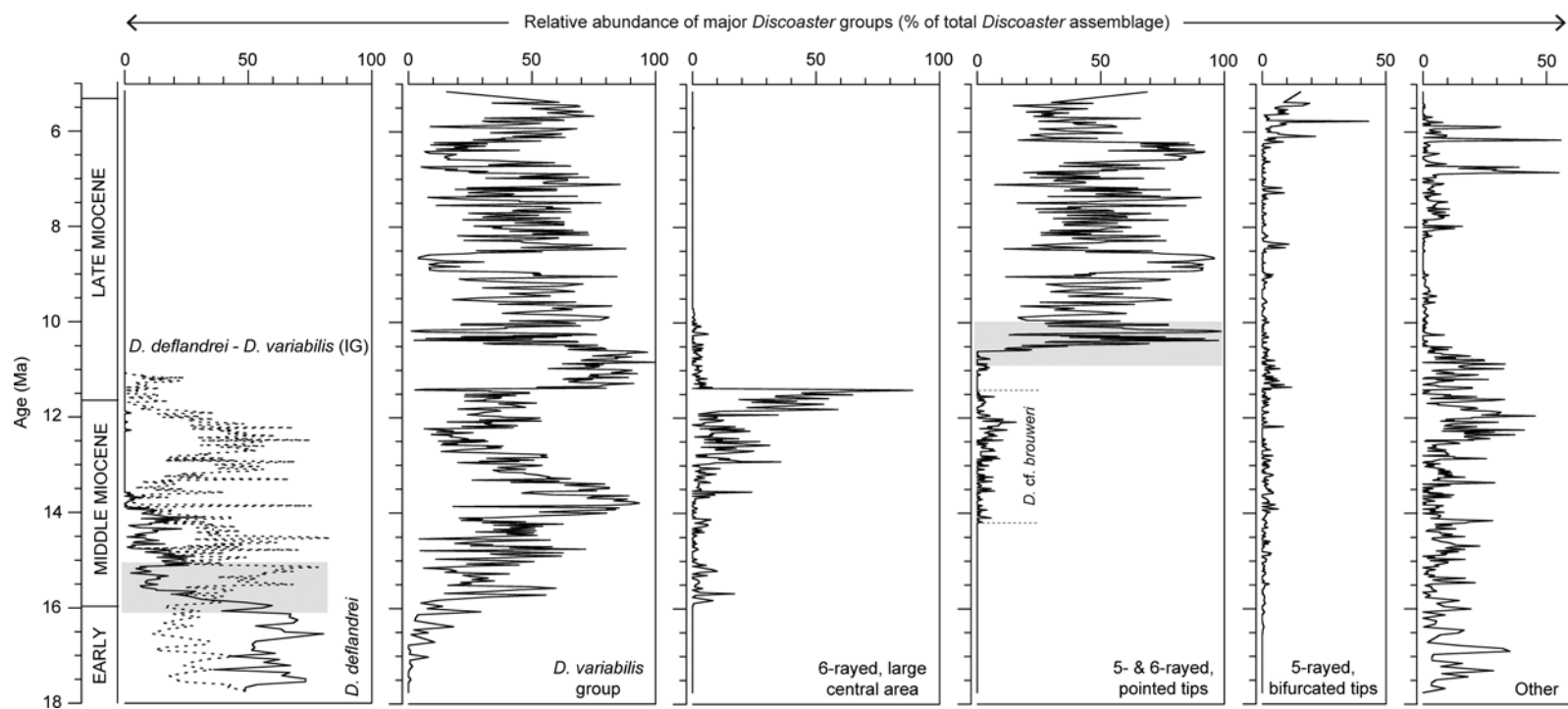


Fig. 11. Relative abundances (%) of major groups of Miocene discoasters from Site U1338 plotted against age. Category 'Other' is composed of unidentified six-rayed discoasters, *D. cf. tristillifer*, *D. triradiatus* and *Discoaster* A, B, C (Backman *et al.* 2013). Transparent grey rectangle over *D. deflandrei* and *D. deflandrei*-*D. variabilis* (IG) panel represents the first major evolutionary transition among Miocene discoasters and the grey rectangle over the panel showing five- and six-rayed discoasters with pointed ray tips represents the second major evolutionary transition among Miocene discoasters.

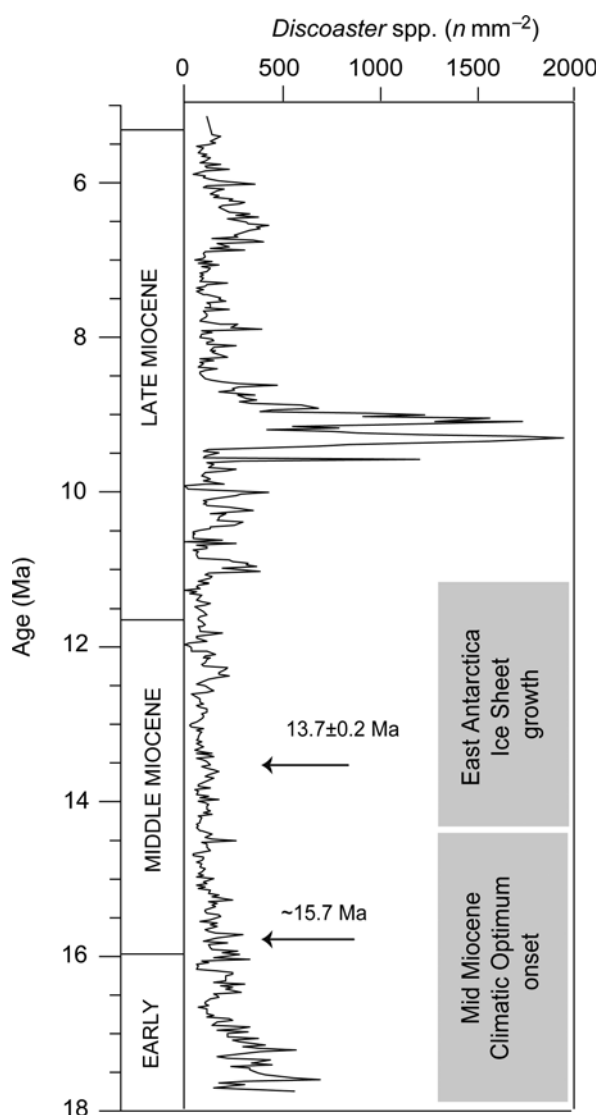


Fig. 12. Total abundance of *Discoaster* spp. ($n \text{ mm}^{-2}$) plotted v. age. The Mid Miocene Climatic Optimum onset and the East Antarctica Ice Sheet growth are indicated by arrows.

Five-rayed discoasters with pointed ray tips include *D. asymmetricus*, *D. bellus*, *D. berggrenii*, *D. quinquaramus*, *D. hamatus* and intergrading forms (Figs 5:8 – 5:16, 9). The simple structure of *D. bellus* represents a new evolutionary development among the late Miocene *Discoaster* populations, that occurred after the long period of dominance of six-rayed forms during the Oligocene and through the early and middle Miocene. *Discoaster bellus* (Fig. 5:8) is the ancestor of three other symmetrical five-rayed discoasters that subsequently evolved during the late Miocene, namely *D. hamatus*, *D. berggrenii* and *D. quinquaramus*. This evolutionary progression is manifested by the presence of specimens showing intermediate morphologies between *D. bellus* and *D. hamatus* (Figs 5:9, 10), and *D. bellus* and *D. berggrenii* (Figs 5:11 – 5:12, 10), respectively, previously noticed also by Rio *et al.* (1990) and Raffi *et al.* (1998).

Discoaster quinquaramus (Fig. 5:15) evolved from *D. berggrenii* through a gradual increase in ray length and decrease in central area size (Raffi *et al.* 1998). The presence of specimens with intergrading morphologies between *D. berggrenii* and *D. quinquaramus* may make the distinction of the two species difficult.

The *D. hamatus* concept used here refers only to five-rayed morphotypes (Figs 5:10, 9), following Perch-Nielsen (1985). Forms

showing intergrading morphologies between *D. bellus* and *D. hamatus* have been recorded just below and along the range of *D. hamatus* (Fig. 10).

Major traits of Miocene discoasters at IODP Site U1338

Above, the abundance patterns of discoasters are plotted v. depth. When summarizing the key trends among these patterns, we consider it useful to plot the data v. age using a low-resolution age model of Site U1338 (Backman *et al.* 2016). Discoasters reveal distinct traits over the late early Miocene through late Miocene interval at Site U1338 (Figs 11 and 12). These features reflect a dynamic evolution within the *Discoaster* genus, characterized by sudden events of speciation/extinction which are of key importance for the biostratigraphic characterization of Miocene. The most prominent among these are:

- (1) the dominance of *D. deflandrei* prior to 15.8 Ma;
- (2) the evolution of and rapid oscillations in relative abundance of the *D. variabilis* group from <20% to over 70% of the total *Discoaster* assemblage in the late Miocene;
- (3) the rapid rise and subsequent decline of six-rayed discoasters having large central areas between 11.4 and 11.8 Ma, there occupying over 46%, on average, of the total *Discoaster* assemblage;
- (4) the rapid rise and subsequent large oscillations in abundance, from <30% to over 60%, of the five- and six-rayed discoasters having pointed ray tips; in terms of relative abundance there is a strong antiphasing relationship (R-value: -0.86) between this group and the *D. variabilis* group;
- (5) the dominance of *D. bellus* between 174.16 and 186.13 m, there occupying over 75%, on average, of the total *Discoaster* assemblage, with peak values of 92% in two samples;
- (6) five samples lack discoasters: 5.83 Ma/92.30 m, 10.36 Ma/218.80 m, 10.83 Ma/235.01 m, 11.38 Ma/253.69 m and 13.73 Ma/331.26 m.

The underlying reason(s) behind these traits remains unclear. Comparisons with palaeoenvironmental proxies such as carbonate content (dissolution), carbon isotopes (productivity) and oxygen isotopes (temperature) provide meagre results. Calculations of correlation coefficients (R) between discoasters and calcium carbonate contents analysed from the identical Site U1338 sample set (Lyle & Backman 2013) show no strong relationship (Fig. 13). Despite large variations in carbonate contents, R-values vary between -0.16 to 0.36 at the species level, and the R-value is 0.25 for the sum of all discoasters (Backman *et al.* 2013). However, when R-values are calculated over 5 – 10 samples in intervals showing low carbonate values due to carbonate dissolution, carbonate content is strongly and positively correlated with low abundances of discoasters.

R-values have been calculated also between partly published (Reghellin *et al.* 2015) and partly unpublished stable isotope (C, O) data from bulk sediment and *Discoaster* abundances at the species level, as well as between these stable isotopes and the sum of all discoasters. Stable isotope and *Discoaster* data are derived from the identical sample set. There are surprisingly low R-values between carbon and oxygen isotopes of bulk sediments on the one hand and abundances of discoasters on the other. R-values for oxygen isotope correlations range from 0.32 to -0.17 , with an average of 0.10 . The sum of all discoasters shows an R-value of 0.05 relative to oxygen isotopes. Carbon isotopes show R-values ranging from 0.09 to -0.27 , with an average of -0.10 . The sum of all discoasters shows an R-value of -0.07 relative to carbon isotopes. If the $\delta^{18}\text{O}$ variations are interpreted as chiefly reflecting temperature in the photic zone environment (as the isotopes mainly represent

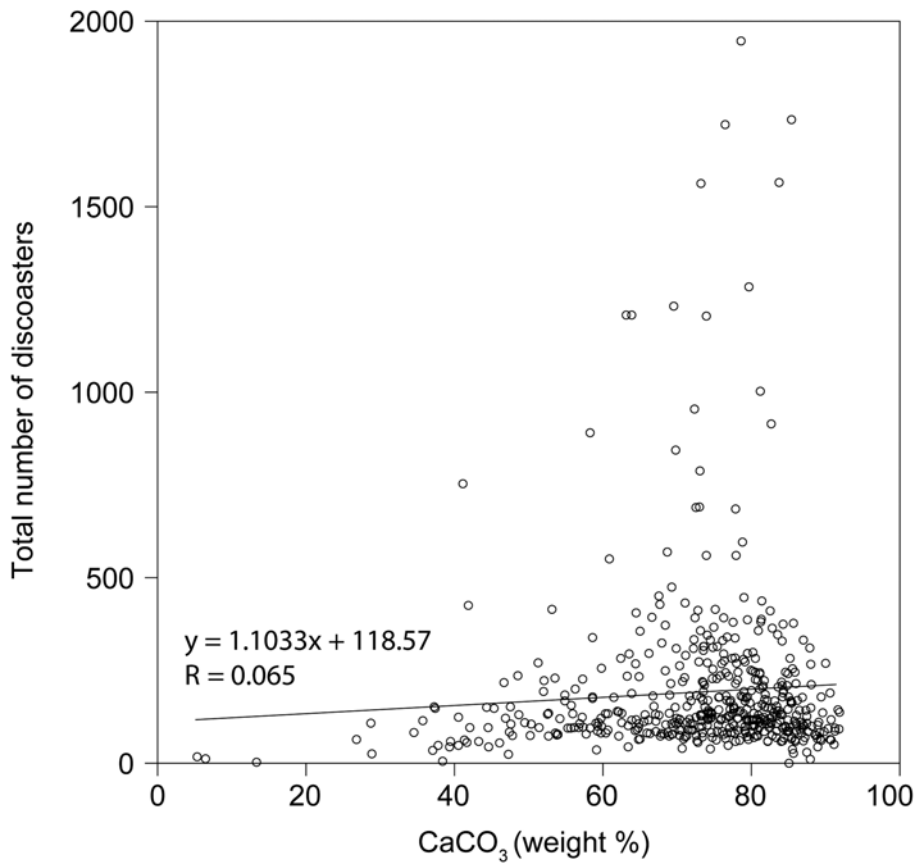


Fig. 13. Plot revealing the poor correlation between total *Discoaster* abundance ($n\text{ mm}^{-2}$) and carbonate content (wt%) at Site U1338. All points over 440 specimens represent *D. bellus*.

nannofossil carbonate; Reghellin *et al.* 2015), the variations in photic zone temperature at Site U1338 had no discernable effect on discoaster abundances. Similarly, if $\delta^{13}\text{C}$ is interpreted as a measure of the intensity of primary productivity in the photic zone environment, the variations in productivity conditions at Site

U1338 had no discernable effect on discoaster abundances. The poor correlation between carbon and oxygen isotopes on the one hand and *Discoaster* abundances on the other is illustrated in Figure 14, using the bulk sediment stable isotope data of Reghellin *et al.* (2015).

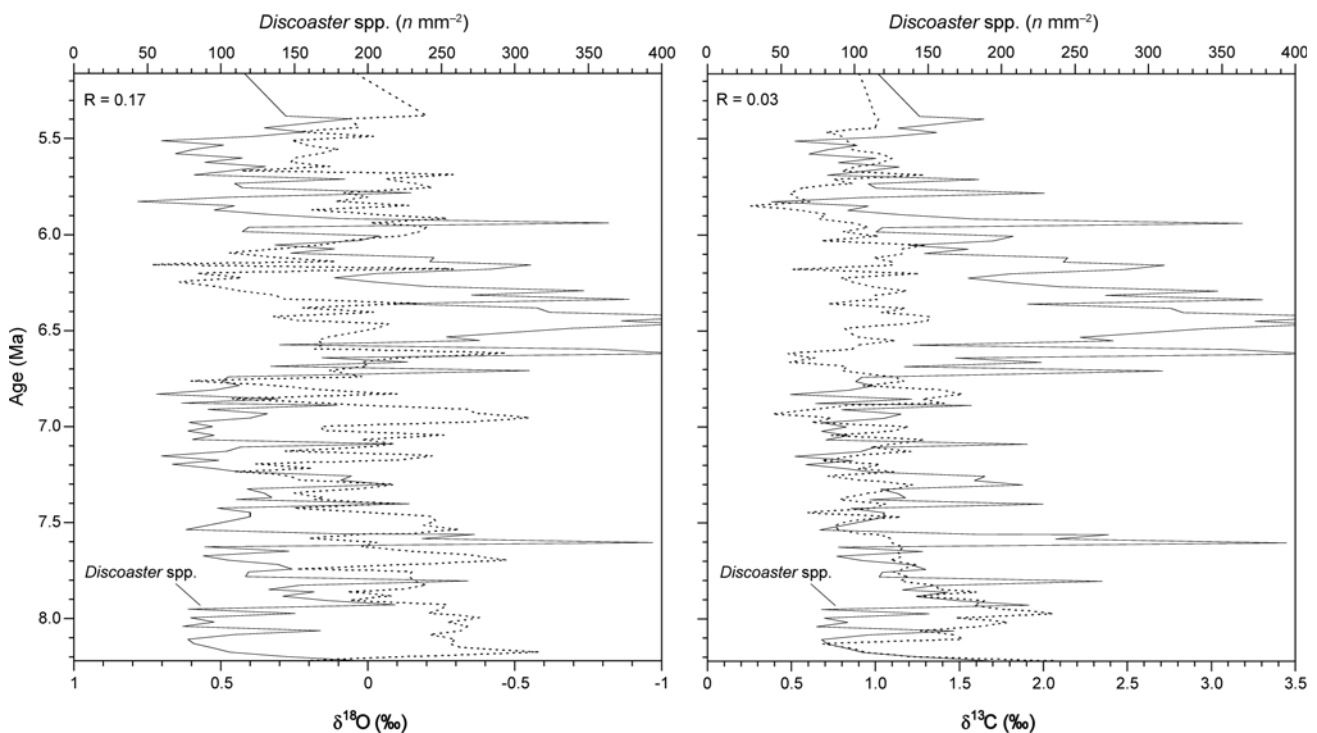


Fig. 14. Plot revealing the poor correlation between total *Discoaster* abundance ($n\text{ mm}^{-2}$) and oxygen isotopes (left panel) and carbon isotopes (right panel). Dotted line represents isotope data (Reghellin *et al.* 2015).

Table 1. Comparison between sampling resolution used in this study, *Chepstow-Lusty et al. (1989, 1992)* and *Gibbs et al. (2004)*

	Site	Sampling resolution (cm)	Sample resolution (ka)
This study	U1338	68	c. 25
<i>Chepstow-Lusty et al. (1989)</i>	552	10	c. 3
	659	10	c. 3
	662	10	c. 3
	607	15	c. 3
	658	30	c. 3
<i>Chepstow-Lusty et al. (1992)</i>	662	10	2
	677	10	c. 0.2
<i>Gibbs et al. (2004)</i>	709	5	c. 0.5
	662	10	c. 3
	926	10	c. 3

These results are at odds with those obtained from the low latitude Atlantic Ocean (*Chepstow-Lusty et al. 1989, 1992; Gibbs et al. 2004*), demonstrating the influence of orbitally forced climatic variation on Pliocene *Discoaster* abundance data. A key difference between our and these Atlantic studies is sample resolution. In our study, sample distances are, on the average, 68 cm, corresponding to a resolution of 1 sample/25 ka in the time domain (Table 1). It appears possible that one cause for the poor correlation between abundance and isotopic oscillations may lie in insufficient sample resolution of our dataset, although other factors may be at play.

The weak correlation between $\delta^{18}\text{O}$, $\delta^{13}\text{C}$ and *Discoaster* abundances could also be explained considering that the isotopic values are calculated on the bulk sediment, which is representative of upper photic zone nannofossil assemblage.

Imai et al. (2015) hypothesized that *Discoaster* were living in the lower photic zone and placoliths in the upper photic zone. Therefore, following this theory, we could supposed that the isotopic signal recorded by the bulk sediment was acquired almost completely from placoliths and not from *Discoaster*, which *Imai et al. (2015)* believes living in deeper waters (lower photic zone). However, there are no concrete scientific evidence supporting the

theory of *Discoaster* being deep water dwellers and, as explained in the introduction, we believe that *Discoaster* prefer warm waters (see also *Edwards 1968; Perch-Nielsen 1972; Bukry 1973a; Haq & Lohmann 1976*). A more scientific approach to explain the ‘isotopic issue’ encountered in this study could be running isotopic analyses on *Discoaster* specimens isolated from the bulk and compare the results with those obtained from both bulk and foraminifera.

Comparing our abundance data with benthic isotope data from Site U1338 (*Holbourn et al. 2014*) suggests that the major decline in abundance of *D. deflandrei* (c. 15.7 Ma) coincides with the onset of the middle Miocene climatic optimum, and that the extinction of this species at 13.7 ± 0.2 Ma coincides with extensive ice growth on Antarctica and a massive increase in opal accumulation at Site U1338 (*Holbourn et al. 2014; Fig. 15*). Their results suggest that climate deteriorated via Antarctic ice growth, which caused intensified upwelling and increased primary productivity in the equatorial Pacific, as manifested at Site U1338. It hence appears tenable to suggest that such a dynamic Miocene photic zone environment strongly influenced *Discoaster* abundances, perhaps even contributed to the well-established evolutionary succession of Miocene *Discoaster*.

Acknowledgements and Funding

We are grateful to Giuliana Villa and Mike Styzen for helpful suggestions in the review of the manuscript. This research used samples and data provided by the Integrated Ocean Drilling Program (IODP). Financial support for data acquisition was provided by Università ‘G. d’Annunzio’ di Chieti-Pescara (Italy) to I Raffi (Fondo Ateneo 2013). J. Backman acknowledges support from Stockholm University and the Swedish Research Council.

Scientific editing by Emanuela Mattioli

References

- Aubry, M.-P. 1984. *Handbook of Cenozoic Calcareous Nannoplankton. Book 1: Ortholithae (Discoasters)*. Micropaleontology Press, American Museum of Natural History, New York.
- Backman, J. & Pestiaux, P. 1987. Pliocene *Discoaster* abundance variations, Deep Sea Drilling Project Site 606: biochronology and paleoenvironmental implications. In: Ruddiman, W.F., Kidd, R.B. & Thomas, E. (eds) *Initial Reports of the Deep Sea Drilling Project*, 94. US Government Printing Office, Washington, DC, 903–910.
- Backman, J. & Shackleton, N.J. 1983. Quantitative biochronology of Pliocene and early Pleistocene calcareous nannofossils from the Atlantic, Indian and Pacific oceans. *Marine Micropaleontology*, 8, 141–170.

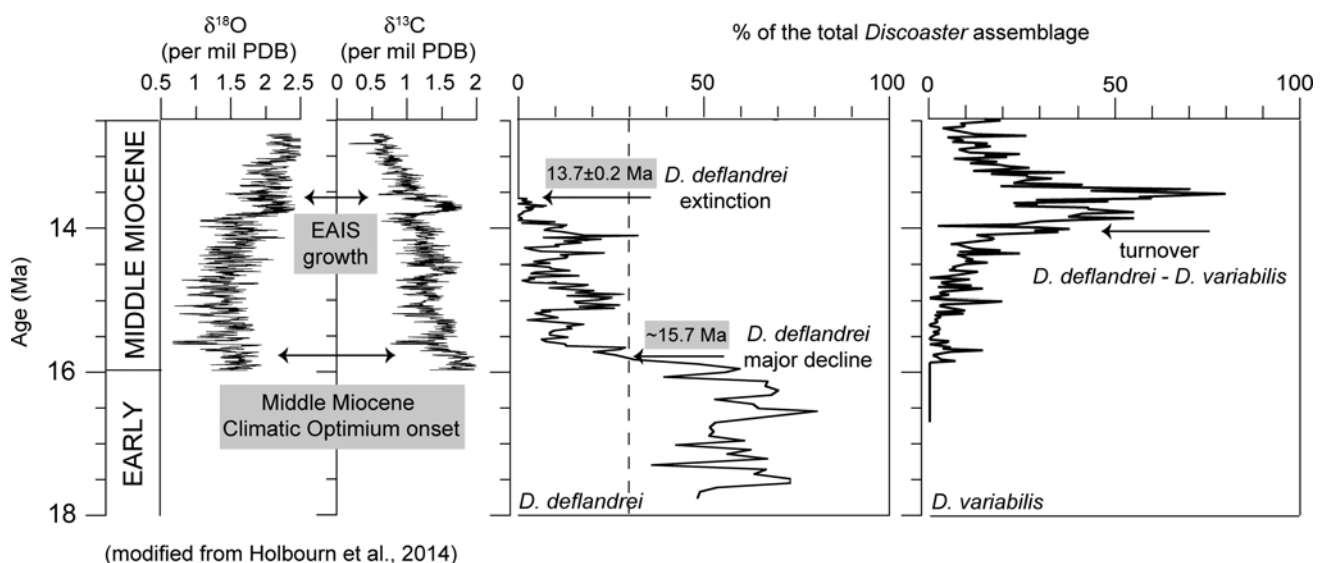


Fig. 15. Comparison between carbon and oxygen isotope curves from Site U1338 (calculated on benthic foraminifera; *Holbourn et al. 2014*) and *Discoaster deflandrei/Discoaster variabilis* relative abundances (%) in the middle Miocene (interval 12.5–16 Ma). *Discoaster deflandrei* major evolutionary steps (decline, extinction and turnover with *Discoaster variabilis*) and their link with the Mid Miocene Climatic Optimum onset and the East Antarctica Ice Sheet (EAIS) growth are indicated with arrows. All plots are v. age.

- Backman, J., Raffi, I., Rio, D., Fornaciari, E. & Pälke, H. 2012. Biozonation and biochronology of Miocene through Pleistocene calcareous nannofossils from low and middle latitudes. *Newsletters on Stratigraphy*, **45**, 221–244.
- Backman, J., Raffi, I., Ciummelli, M. & Baldauf, J. 2013. Species-specific responses of late Miocene *Discoaster* spp. to enhanced biosilica productivity in the equatorial Pacific and the Mediterranean. *Geo-Marine Letters*, **33**, 285–298.
- Backman, J., Baldauf, J.G., Ciummelli, M. & Raffi, I. 2016. Data report: a revised biomagnetostratigraphic age model for Site U1338, IODP Expedition 320/321. In: Pälke, H., Lyle, M., Nishi, H., Raffi, I., Gamage, K., Klaus, A. & the Expedition 320/321 Scientists *Proceedings of the Integrated Ocean Drilling Program*, **320/321**. Integrated Ocean Drilling Program Management International, Tokyo, <http://doi.org/10.2204/iodp.proc.320321.219.2016>
- Baldauf, J.G. & Barron, J.A. 1990. Evolution of biosiliceous sedimentation patterns for the Eocene through Quaternary: Paleooceanographic response to polar cooling. In: Thiede, J. & Bleil, U. (eds) *Geologic history of the polar oceans: Arctic versus Antarctic*. NATO ASI Ser. C, Kluwer, Dordrecht, 575–608.
- Bown, P.R. & Young, J.R. 1998. Techniques. In: Bown, P.R. (ed.) *Calcareous Nannofossil Biostratigraphy*. Kluwer Academic, Dordrecht, 16–28.
- Bramlette, M.N. & Riedel, W.R. 1954. Stratigraphic value of discoasters and some other microfossils related to Recent coccolithophores. *Journal of Paleontology*, **28**, 385–403.
- Bukry, D. 1971a. Cenozoic calcareous nannofossils from the Pacific Ocean. *Transactions of the San Diego Society of Natural History*, **16**, 303–327.
- Bukry, D. 1971b. *Discoaster* evolutionary trends. *Micropaleontology*, **17**, 43–52.
- Bukry, D. 1973a. Coccolith stratigraphy, eastern equatorial Pacific, Leg 16, Deep Sea Drilling Project. In: van Andel, T.H. & Heath, G.R. (eds) *Initial Reports of the Deep Sea Drilling Project*, **16**. US Government Printing Office, Washington, DC, 653–711.
- Bukry, D. 1973b. Low-latitude coccolith biostratigraphic zonation. In: Edgar, N.T. & Saunders, J.B. (eds) *Initial Reports of the Deep Sea Drilling Project*, **15**. US Government Printing Office, Washington, DC, 685–703.
- Bukry, D. 1981. Pacific coast coccolith stratigraphy between Point Conception and Cabo Corrientes, Deep Sea Drilling Project Leg 63. In: Yeats, R.S. & Haq, B.U. (eds) *Initial Reports of the Deep Sea Drilling Project*, **63**. US Government Printing Office, Washington, DC, 445–471.
- Bukry, D. & Percival, S.F. Jr. 1971. New Tertiary calcareous nannofossils. *Tulane Studies in Geology and Paleontology*, **8**, 123–146.
- Chepstow-Lusty, A., Backman, J. & Shackleton, N.J. 1989. Comparison of upper Pliocene *Discoaster* abundance variations from North Atlantic Sites 552, 658, 659, and 662: Further evidence for marine plankton responding to orbital forcing. In: Ruddiman, W.F. & Samtheim, M. (eds) *Proceedings of the ODP, Scientific Results*, **108**. Ocean Drilling Program, College Station, TX, 121–114.
- Chepstow-Lusty, A., Shackleton, N.J. & Backman, J. 1992. Upper Pliocene *Discoaster* abundance from the Atlantic, Pacific, and Indian oceans: the significance of productivity pressure at low latitudes. *Memorie di Scienze Geologiche Padova*, **44**, 357–373.
- Edwards, A.R. 1968. The calcareous nannoplankton for Tertiary New Zealand climates. *Tuatara*, **16**, 26–31.
- Filewicz, M.V. 1985. Calcareous nannofossil biostratigraphy of the Middle America Trench and slope, Deep Sea Drilling Project Leg 84. In: von Huene, R. & Aubouin, J. (eds) *Initial Reports of the Deep Sea Drilling Project*, **84**. US Government Printing Office, Washington, DC, 339–361.
- Furrazzola-Bermúdez, G. & Itturalde, V.M. 1967. Estudio micropaleontológico del Oligoceno superior de Cuba, en el pozo Pijuan No. 47. *Tecnologica*, **5**, 3–11.
- Gartner, S. 1967. Calcareous nannofossils from Neogene of Trinidad, Jamaica, and Gulf of Mexico. *University of Kansas Paleontological Contributions*, **29**, 1–7.
- Gibbs, S., Shackleton, N. & Young, J. 2004. Orbitally forced climate signals in mid-Pliocene nannofossil assemblages. *Marine Micropaleontology*, **51**, 39–56.
- Haq, B.U. & Lohmann, G.P. 1976. Early Cenozoic calcareous nannoplankton biogeography of the Atlantic Ocean. *Marine Micropaleontology*, **1**, 119–194.
- Hay, W.W., Mohler, H.P., Roth, P.H., Schmidt, R.R. & Boudreaux, J.E. 1967. Calcareous nannoplankton zonation of the Cenozoic of the Gulf coast and Caribbean-Antillean area and Transoceanic correlation. *Transactions of the Gulf Coast Association of Geological Societies*, **17**, 428–459.
- Holbourn, A., Kuhnt, W., Lyle, M., Schneider, L., Romero, O. & Andersen, N. 2014. Middle Miocene climate cooling linked to intensification of eastern equatorial Pacific upwelling. *Geology*, **42**, 19–22.
- Holden, N.E., Bonardi, M.L., De Bièvre, P., Renne, P.R. & Villa, I.M. 2011. IUPAC-IUGS common definition and convention on the use of the years as a derived unit of time (IUPAC Recommendations 2011). *Pure and Applied Chemistry*, **23**, 1159–1162.
- Imai, R., Farida, M., Sato, T. & Iryu, Y. 2015. Evidence for eutrophication in the northwestern Pacific and eastern Indian oceans during the Miocene to Pleistocene based on the nannofossil accumulation rate, *Discoaster* abundance, and coccolith size distribution of Reticulofenestra. *Marine Micropaleontology*, **116**, 15–27.
- Kennett, J.P. & Srinivasan, M.S. 1983. *Neogene Planktonic Foraminifera – A Phylogenetic Atlas*. Hutchinson Ross.
- Lohmann, G.P. & Carlson, J.J. 1981. Oceanographic significance of Pacific late Miocene calcareous nannoplankton. *Marine Micropaleontology*, **6**, 553–579.
- Lourens, L.J., Hilgen, F.J., Shackleton, N.J., Laskar, J. & Wilson, D. 2004. The Neogene Period. In: Gradstein, F.M., Ogg, J.G. & Smith, A.G. (eds) *A Geological Time Scale 2004*. Cambridge University Press, Cambridge, 409–440.
- Lyle, M. & Backman, J. 2013. Data Report: Calibration of XRF-estimated CaCO₃ along the Site U1338 splice. In: Pälke, H., Lyle, M., Nishi, H., Raffi, I., Gamage, K. & Klaus, A. (eds) *Proceedings of the Integrated Ocean Drilling Program*, **320/321**. Integrated Ocean Drilling Program Management International, Tokyo, 1–16. <http://doi.org/10.2204/iodp.proc.320321.205.2013>
- Martini, E. & Bramlette, M.N. 1963. Calcareous nannoplankton from the experimental mohole drilling. *Journal of Paleontology*, **37**, 845–856.
- Moore, T.C., Backman, J., Raffi, I., Nigrini, C., Sanfilippo, A., Pälke, H. & Lyle, M. 2004. Paleogene tropical Pacific: Clues to circulation, productivity and plate motion. *Paleoceanography*, **19**(PA3013), 1–16.
- Moshkovitz, S. & Ehrlich, A. 1980. Distribution of the calcareous nannofossils in the Neogene sequence of the Jaf-fa-1 Borehole, Central Coastal Plain. *Geological Survey of Israel Report*, **PD/1/80**, 1–25.
- Okada, H. & Bukry, D. 1980. Supplementary modification and introduction of code numbers to the low-latitude coccolith biostratigraphic zonation (Bukry, 1973; 1975). *Marine Micropaleontology*, **5**, 321–325.
- Pälke, H., Lyle, M., Nishi, H., Raffi, I., Gamage, K. & Klaus, A. 2010. *Pacific equatorial age transect. Proceedings of the Integrated Ocean Drilling Program*, **320/321**. Integrated Ocean Drilling Program Management International, Tokyo, <http://doi.org/10.2204/iodp.proc.320321.2010>
- Pennington, J.T., Mahoney, K.L., Kuwahara, V.S., Kolber, D.D., Calienes, R. & Chavez, F.P. 2006. Primary production in the eastern tropical Pacific: A review. *Progress in Oceanography*, **69**, 285–317.
- Perch-Nielsen, K. 1972. Remarks on late Cretaceous to Pleistocene coccoliths from the North Atlantic. In: Loughton, A.S. & Berggren, W.A. (eds) *Initial Reports of the Deep Sea Drilling Project*, **12**. US Government Printing Office, Washington, DC, 1003–1069.
- Perch-Nielsen, K. 1985. Cenozoic calcareous nannofossils. In: Bolli, H.M., Saunders, J.B. & Perch Nielsen, K. (eds) *Plankton Stratigraphy*. Cambridge University Press, Cambridge, 427–554.
- Prins, B. 1971. Speculations on relations, evolution, and stratigraphic distribution of discoasters. In: Farinacci, A. (ed.) *Proceedings of the II Planktonic Conference*. Edizione Tecnoscienza, Roma, 1017–1037.
- Raffi, I. & Flores, J.A. 1995. Pleistocene through Miocene calcareous nannofossils from Eastern Equatorial Pacific Ocean (Leg 138). In: Piasis, N.G., Mayer, L.A., Janecek, T.R., Palmer-Julson, A. & van Andel, T.H. (eds) *Proceedings of the ODP, Scientific Results*, **138**. Ocean Drilling Program, College Station, TX, 233–286.
- Raffi, I., Rio, D., d'Atri, A., Fornaciari, E. & Rocchetti, S. 1995. Quantitative distribution patterns and biomagnetostratigraphy of middle and late Miocene calcareous nannofossils from equatorial Indian and Pacific oceans (Legs 115, 130, and 138). In: Piasis, N.G., Mayer, L.A., Janecek, T.R., Palmer-Julson, A. & van Andel, T.H. (eds) *Proceedings of the ODP, Scientific Results*, **138**. Ocean Drilling Program, College Station, TX, 479–502.
- Raffi, I., Backman, J. & Rio, D. 1998. Evolutionary trends of tropical calcareous nannofossils in the late Neogene. *Marine Micropaleontology*, **35**, 17–41.
- Raffi, I., Backman, J., Fornaciari, E., Pälke, H., Rio, D., Lourens, L. & Hilgen, F. 2006. A review of calcareous nannofossil astrochronology encompassing the past 25 million years. *Quaternary Science Reviews*, **25**, 3113–3137.
- Reghellin, D., Coxall, H.K., Dickens, G.R. & Backman, J. 2015. Carbon and oxygen isotopes of bulk carbonate in sediment deposited beneath the eastern equatorial Pacific over the last 8 million years. *Paleoceanography*, **30**, 1261–1286. <http://doi.org/10.1002/2015PA002825>
- Rio, D., Fornaciari, E. & Raffi, I. 1990. Late Oligocene through early Pleistocene calcareous nannofossils from western equatorial Indian Ocean (Leg 115). In: Duncan, R.A., Backman, J. & Peterson L.C. (eds) *Proceedings of the ODP, Scientific Results*, **115**. Ocean Drilling Program, College Station, TX, 175–235.
- Roth, P.H. & Thierstein, H. 1972. Calcareous nannoplankton: Leg 14 of the Deep Sea Drilling Project. In: Hayes, D.E. & Pimm, A.C. (eds) *Initial Reports of the Deep Sea Drilling Project*, **14**. US Government Printing Office, Washington, DC, 421–485.
- Stradner, H. 1959. First report on the discoasters of the Tertiary of Austria and their stratigraphic use. In: *Proceedings of the 5th World Petroleum Congress*, New York, 1081–1095.
- Stradner, H. 1973. Catalogue of calcareous nannoplankton from sediments of Neogene age in the eastern North Atlantic and Mediterranean Sea. In: Ryan, W.B.F. & Hsu, K.J. (eds) *Initial Reports of the Deep Sea Drilling Project*, **13**. US Government Printing Office, Washington, DC, 1137–1199.
- Takayama, T. 1969. Discoasters from the Lamont Core V21–98 (preliminary reports of the Philippine sea cores. Part 2). *Bulletin of the National Science Museum*, **12**, 431–450.
- Theodoridis, S. 1984. Calcareous nannofossil biozonation of the Miocene and revision of the helicoliths and discoasters. *Utrecht Micropaleontological Bulletin*, **32**, 1–271.
- Wei, W. & Wise, S.W. Jr. 1990. Biogeographic gradients of middle Eocene–Oligocene calcareous nannoplankton in the South Atlantic Ocean. *Palaeogeography Palaeoclimatology Palaeoecology*, **79**, 29–61.
- Wilkins, R.H., Dickens, G.R., Tian, J. & Backman, J. & Expedition 320/321 Scientists 2013. Data report: revised composite depth scales for Sites U1336, U1337, and U1338. In: Pälke, H., Lyle, M., Nishi, H., Raffi, I., Gamage, K. & Klaus, A. (eds) *Proceedings of the Integrated Ocean Drilling Program*, **320/321**. Integrated Ocean Drilling Program Management International, Tokyo, 1–158.
- Young, J.R. 1998. Neogene. In: Bown, P.R. (ed.) *Calcareous Nannofossil Biostratigraphy*. Kluwer Academic, Dordrecht, 225–265.
- Zachos, J.C., Pagani, M., Sloan, L., Thomas, E. & Billups, K. 2001. Trends, rhythms, and aberrations in global climate 65 Ma to present. *Science*, **292**, 686–693.